Attention to Safety 2

P.J. Ward

J.C.J.H. Aerts

S.C. van Pelt

O. de Keizer

B.J.J.M. van den Hurk

J.J Beersma

T.A. Buishand

Adaptation

climate changes
spatial planning

Attention to Safety 2

Authors

P.J. Ward [1,2]
J.C.J.H. Aerts [1,2]
S.C. van Pelt [3,4]
O. de Keizer [5]
B.J.J.M. van den Hurk [3]
J.J Beersma [3]
T.A. Buishand [3]

1 Institute for Environmental Studies (IVM), VU University Amsterdam
2 Amsterdam Global Change Institute (AGCI), VU University Amsterdam
3 Royal Netherlands Meteorological Institute (KNMI)
4 Earth System Science Group, Wageningen University and Research Centre
5 Deltares

IVM Institute for Environmental Studies

AGCI Amsterdam Global Change Institute

WAGENINGEN UNIVERSITY
WAGENINGEN UR

Royal Netherlands Meteorological Institute
Ministry of Infrastructure and the Environment

Deltares
Enabling Delta Life

Contents

Summary

Summary in Dutch

Tot op heden heeft onderzoek naar toekomstig overstromingsrisico vooral gebruik gemaakt van de scenarioaanpak. Het belangrijkste doel van deze studie is om een demonstratie te geven van een methode voor het produceren van probabilistische schattingen van overstromingsrisico's als gevolg van klimaatverandering. Het onderzoek richt zich op twee casestudy trajecten langs de Rijn: Bonn-Duisburg en Mainz-Koblenz.

Eerst hebben we een ensemble van lange (3000-jaar) geresampelde tijdreeksen van klimaatvariabelen gegenereerd op basis van 12 GCM simulaties. Aan dit ensemble hebben we een ensemble van zes RCM simulaties toegevoegd uit het RheinBlick 2050 project. Deze zijn gebruikt in het hydrologische model HBV-96 om rivierafvoer te simuleren. Daarna is een schatting gemaakt van extreme afvoerkwantielen per klimaattijdreeks voor herhalingstijden tot 3000 jaar. Om van extreme rivierafvoeren tot overstromingsschade- en risico te komen hebben we een eenvoudig inundatiemodel ontwikkeld (Floodscanner), en dit gekoppeld aan een overstromingsschademodel (Damagescanner).

Met deze aanpak hebben we probabilistische overstromingsrisico scenario's ontwikkeld. Hiermee kunnen we de kans schatten dat een toekomstig overstromingsrisico hoger is dan het huidige risico (binnen de grenzen van deze studie), namelijk: 92% voor het gebied Bonn-Duisburg en 96% voor het gebied Mainz-Mosel. Met deze methode kan de kans worden geschat dat een overstromingsrisico hoger wordt, wat een evaluatie van risico onder extreme toekomstige situaties mogelijk maakt.

Summary

To date, flood risk research has predominantly relied on a discrete scenario-based approach. In the present study we demonstrate a framework for producing probabilistic estimates of flood risk under climate change, focussing on two case-study stretches of the Rhine: Bonn-Duisburg and Mainz-Koblenz.

We used an ensemble of six (bias-corrected) RCM future simulations to create a 3000-yr time-series through resampling. This was complemented with 12 GCM-based future time-series, constructed by resampling observed climate time-series and modifying these to represent future conditions using an advanced delta-change approach. The resampled time-series were used as input in the hydrological model HBV-96 to simulate discharge, and extreme discharge quantiles were estimated. To convert extreme discharges to estimates of flood damage and flood risk, we developed a simple inundation model (Floodscanner), and coupled this with a flood damage model (Damagescanner).

Using this approach, we developed probabilistic flood risk scenarios. This allows us to estimate the probability of future flood risk exceeding current risk (given the limitations of the study), namely: 92% for the section Bonn-Duisburg and 96% for the section Mainz-Mosel. Using such a framework it is possible to assess the probability that flood risk will increase by any given factor, allowing for the assessment of risk under possible extreme future scenarios.

Extended summary

Background

To date, future flood risk assessments have predominantly relied on a discrete scenario-based approach. This is also the case in climate change impact assessments in general. The discrete scenarios approach is useful for exploring potential impacts of climate change, but presents problems for assessing the effectiveness of adaptation options. Recent research proposes a probabilistic approach, generating probability density functions (PDFs) of climate change. Next to research on probabilistic climate change scenarios, the climate impacts community has expressed the need for probabilistic impact assessments. In the Netherlands, the project Attention for Safety (AvV), as well as the report of the Veerman Commission (www.deltacommissie.com), recommended the development of such methods for probabilistic flood risk assessments. The present study responds to this, and is the first attempt to assess future flood risk under climate change in a probabilistic framework.

Aims and objectives

The main aim of this research is to provide a demonstration of a framework for producing probabilistic estimates of flood risk, and to demonstrate how ensembles of climate projections can be constructed and used for this purpose.

The main objectives are:
- To generate long resampled time-series of climate variables and discharge for use in probabilistic flood risk assessments;
- To develop probability density functions of extreme discharge under climate change;
- To develop a rapid inundation model capable of providing the large number of inundation maps needed in probabilistic flood risk assessments, and to couple this with a flood damage model;
- To demonstrate the production of flood risk estimates in a probabilistic framework.

Setup of main report

The main part of this synthesis report is set up as follows. In Section 1 we discuss the background to the study and the aims and objectives. In Section 2 we describe the study area, followed in Section 3 with methods and data used in the project. Section 4 describes the results of a pilot study carried out to develop and validate the new inundation model; the pilot study was carried out for the Meuse River in Dutch Limburg, since relatively good data are available for model testing and validation. In this section we also present a limited validation for the Rhine basin. In Section 5 we present the results of the probabilistic flood risk analyses for two case-study stretches of the Rhine in Germany, namely: (a) Bonn-Duisburg; and (b) Mainz-Koblenz. In Section 6 we discuss the findings, limitations, and future research needs, and finally we provide conclusions in Section 7.

Study area

The probabilistic flood risk assessment focuses on two case-study stretches of the Rhine River in Germany, namely the sections: (a) Bonn-Duisburg; and (b) Mainz-Koblenz. The Rhine is one of the most important industrial transport routes in the world, and about 58 million people inhabit the river basin, of which an estimated 10.5 million live in flood-prone areas. Many studies have assessed how climate change may alter the discharge regime of the River Rhine. These studies suggest that mean winter discharge at Lobith (border Germany-Netherlands) may increase by 0 to 30% by 2050, while mean summer discharge may change by -45 to +15%. Moreover, the magnitude of extreme flood events is generally projected to increase. However, the assessment of current and future flood risk in the basin is still in its early phases.

Developing long time-series of climate variables and discharge for use in probabilistic flood risk assessments

For this research, bias-corrected, resampled time-series of 3000 years from an ensemble of six Regional Climate Model (RCM) simulations were made available through the RheinBlick 2050 project. Some of the RCM simulations used in RheinBlick 2050 were driven by the same General Circulation Model (GCM) simulation or by an alternative simulation run or version of the same GCM. In order to enlarge the number of GCMs in our ensemble, 12 GCM simulations run in the context of the 3rd Coupled Model Intercomparison Project (CMIP3) were downscaled using an advanced delta-change approach. The GCM simulations used were all driven by the Intergovernmental Panel on Climate Change (IPCC) Special Report on Emission Scenarios (SRES) A1B emission scenario.

Representative time-series of the future GCM climates were obtained by transforming a 3000-year resampled sequence of daily precipitation and temperature from historical observations for the period 1961-1995 from the International Commission for the Hydrology of the Rhine basin (CHR) reference dataset. An advanced delta method was used taking into account the changes in extreme rainfall and temperature variability as well as the changes in their means. The resampling algorithm in this study, which can be regarded as a weather generator, is the same as that used in the RheinBlick 2050 project. The hydrological model HBV-96 was then forced with the 3000-year time-series for the 12 GCM and six RCM simulations to derive 3000-year synthetic sequences of daily discharge. Discharge quantiles for the different flood return periods were estimated using the Weissman approach.

The winter half-year maximum 10-day basin-average precipitation sums were analysed, because these events often cause high discharge in the lower part of the Rhine basin. The GCM ensemble showed higher quantiles of winter half-year maximum 10-day basin-average precipitation sums than in the RCM future ensemble for each return period. The spread between the estimated quantiles of winter half-year maximum 10-day basin-average precipitation sums for the RCM future ensemble members increases as the return periods become longer. For the extreme discharge events, the bandwidths of the two ensembles are similar at Lobith and Cologne, but the bandwidth of the RCM ensemble is smaller than that of the GCM ensemble at Kaub. We also found interesting spatial differences in the results. For example, the climate model ensemble members do not cause the same changes in extreme discharge in all parts of the basin. This demonstrates the importance of using spatially distributed climate simulations when carrying out climate change impact studies.

The results show that adding the ensemble of 12 GCM members to the existing ensemble of six RCM members (driven by four parent GCMs) from RheinBlick 2050 leads to a relatively small increase in the overall spread of the extreme discharge results, although the ensemble means of the estimated discharge quantiles appear to be greater for the GCM ensemble. It must therefore be concluded that the 6 RCMs used have a considerable influence on the climate, and therefore discharge, projections.

Developing an inundation model capable of providing the large number of inundation maps needed in probabilistic flood risk assessments

A hindrance to probabilistic flood risk modelling has been the large number of inundation maps required, since for each ensemble member and/or scenario, damage estimates must be made for several flood return periods, each with a different associated inundation depth and extent. Generally, the production of flood hazard maps is very time-consuming and computationally expensive. In this project, we developed a rapid flood inundation model (Floodscanner), coupled to an existing flood damage model (Damagescanner). The Floodscanner model appears to perform fairly well in both the Rhine and Meuse basins, but the simplifications used dictate its application. The Floodscanner method is certainly not intended to replace the need for hydraulic modelling with more complex

models. The approach is neither suitable for localised flood risk assessments (e.g. street to city scale), nor for presenting flood risk at the grid-cell level. Rather, the approach is intended to be complementary to state-of-the-art methods for use in regional-to-basin scale studies in which large numbers of inundation maps are required. More attention is needed to the development of relatively simple inundation models. The method developed and applied here is capable of this, but refinements could be added to include the most important physical processes in a simple manner.

Flood risk estimates in a probabilistic framework

Flood damage was calculated using the Damagescanner model, which uses the inundation maps from Floodscanner to estimate direct economic damage per inundation scenario. For each climate model ensemble member, damage was estimated for all flood return periods from 200 to 3000 years (with a step of 10 years). Flood risk, or expected annual loss, was then estimated as the area under the exceedance probability-loss curve (risk curve). A risk curve was developed for the reference climate (resampled observations, representative of the period 1961-1995), and also for the future climate for each GCM/RCM ensemble member (representative of the period 2081-2100).

The individual estimates of flood risk per ensemble member were used to derive probability density functions (PDFs) of risk for the RCM ensemble, the GCM ensemble, and the full ensemble (i.e. all future GCM and RCM ensemble members combined). We applied a two-parameter gamma distribution to the individual risk estimates within each future ensemble, whereby each ensemble member was assumed to have an equal likeliness (i.e. no weighting was carried out). Our analyses allow us to estimate the probability of future flood risk exceeding current risk (given the limitations of the study), namely: 92% for the section Bonn-Duisburg and 96% for the section Mainz-Mosel. By extension, using such a framework it is possible to assess the probability that flood risk will increase by any given factor, allowing for the assessment of risk under possible extreme future scenarios.

The range between the maximum and minimum risk estimate is slightly larger in the GCM ensemble than in the RCM ensemble for both case-study areas, although the standard deviation is smaller. However, the differences between both ensembles are small and may be partly related to the difference in ensemble size. The addition of the GCM ensemble to the existing RCM ensemble from RheinBlick 2050 leads to an increase in the spread of the PDF, and also leads to a higher mean estimate of flood risk. Whilst the results show that the RCMs in our ensembles have a major impact on the climate, discharge, and risk projections, the analyses do not allow for a more general statement of the relative influence of RCMs and GCMs on these variables.

Future research

This project presents the first assessment of future flood risk under scenarios of climate change in a probabilistic framework. It is intended to give a demonstration of the methods that can be used in such a framework. The absolute figures should be used for qualitative comparison only in decision-making at this time. Probabilistic flood risk assessments hold promise, but research remains to be carried out to: refine the methods presented here; examine how the methods can be applied to improve adaptation planning; assess how decision-makers use results of probabilistic impacts assessments; and to investigate how the information provided can most effectively be communicated to stakeholders.

1. Introduction

Traditionally, flood management has concentrated on providing protection against floods through technical measures aimed at reducing the probability of flooding, such as dikes, river straightening, and retention by reservoirs [e.g. Merz et al., 2010a; Vis et al., 2003]. Due to climate change, the intensity and/or frequency of flooding is projected to increase in the future in many parts of the world [IPCC, 2007a]. The same tendency is found for the middle and lower part of the international Rhine basin [Görgen et al., 2010]. This means that technical measures of flood protection would need to be constantly upgraded in order to comply with designated safety standards. Moreover, recent studies on trends in losses due to weather-related natural disasters show that the observed increases in damage over the last century are, in fact, caused primarily by an increasing exposure of population and capital to floods [Bouwer, 2010]. Therefore, flood management should not only aim to reduce the probability of flooding, but also to reduce the impacts if a flood occurs. Indeed, international water management is increasingly shifting towards a more integrated system of flood risk management [Few, 2003; Merz et al., 2010a; Tunstall et al., 2004], whereby flood risk is defined as the probability of flooding multiplied by the potential consequences [Kron, 2005].

In economic terms, flood risk can be expressed as the expected annual loss [e.g. Meyer et al., 2009]. In order to calculate (potential) flood damage (or loss) for a given flood event, the most common approach involves combining data on the characteristics of the event (hazard) with information on the assets that would be exposed to it (exposure), and information about the vulnerability of those exposed assets to the particular hazard [e.g. De Moel and Aerts, 2011; Kron, 2005; Merz et al., 2010b]. In these studies, hazard is represented by hazard-maps, showing certain flood characteristics (per grid-cell) related to a particular flood, for example inundation depth, flow velocity, inundation duration, and sediment or contamination load. Exposure is often represented by land use maps, whereby each land use class is assigned an economic value per hectare. Finally, vulnerability is most commonly represented by depth-damage functions, which show the amount of damage that would occur per hectare for each land use class and for different inundation depths [e.g. Merz et al., 2010b].

To date, future flood risk assessments have predominantly relied on a discrete scenario-based approach [e.g. IPCC, 2007a]. This is not only the case in flood risk assessment, but also in climate change impact assessments in general. The discrete scenarios approach is useful for exploring potential impacts of climate change, but presents problems for assessing the effectiveness of adaptation options [New et al., 2007]. Recent research proposes a probabilistic approach, generating probability density functions (PDFs) of climate change [e.g. Fowler et al., 2005; Rougier, 2007; Tebaldi et al., 2004]. Potentially, large ensembles of General Circulation Model (GCM) and Regional Climate Model (RCM) simulations (containing, for example, hundreds of ensemble members), could provide more information on risk and uncertainty than using a limited number of discrete scenarios [New et al., 2007]. Next to research on probabilistic climate change scenarios, the climate impacts community has expressed the need for probabilistic impact assessments [e.g. Pittock et al., 2001; Reilly et al., 2001; Tebaldi et al., 2004; Webster, 2003]. Examples of probabilistic climate impact studies exist in several fields, including: global crop yields [Tebaldi and Lobell, 2008]; water resources management [Manning et al., 2009; New et al., 2007]; and storm surge impacts [Gaslikova et al., 2011].

In the Netherlands, the project Attention for Safety (AvV) [Aerts et al., 2008], as well as the report of the Veerman Commission (www.deltacommissie.com), recommended the development of methods for probabilistic flood risk assessments. To date, the only probabilistic flood risk framework is that of Apel et al. [2006], in which a simple stochastic approach allowing a large number of simulations in a Monte Carlo framework provided the basis for a probabilistic risk assessment for an area of the

Rhine (between Cologne and Rees, with a focus on the polder at Mehrum). However, their study only examines probabilistic risk assessments based on current climate observations, and does not develop scenarios of flood risk under future climate change. In the AvV2 project, we describe such an assessment for the first time.

A hindrance to probabilistic flood risk modelling is the number of inundation maps required, since for each ensemble member and/or scenario, damage estimates must be made for several flood return periods, each with a different associated inundation depth and extent. Generally, the production of flood hazard maps is very time-consuming and computationally expensive [Apel et al., 2008; Gouldby and Kingston, 2007; Woodhead et al., 2007]. Even relatively simple 1D and coupled 1D-2D models run on the order of minutes to hours for river-stretches of the order of magnitude 10-100 km, whilst full 2D or 3D models may take several days [e.g. Woodhead et al., 2007]. Hence, inundation mapping models are required that are capable of rapidly simulating inundation extent and depth. Ideally, these would also be dynamically coupled to models for estimating the associated flood damage. In this project, we developed a rapid flood inundation model, coupled to an existing flood damage model.

The estimation of the probabilities (or return periods) of extreme flood events is also far from trivial. For current climate conditions, frequency analysis is often applied on historical discharge series, which requires the extrapolation of fitted extreme value distributions [Garrett and Müller, 2008]. More sophisticated approaches combine weather generators with hydrological models to create such long discharge series that extrapolation is redundant. For the Rhine basin, a multi-site weather generator has been developed based on non-parametric resampling [Buishand and Brandsma, 2001, Wójcik et al., 2000]. This resampling technique has recently been applied to RCM data for the Rhine basin in the RheinBlick 2050 project [Görgen et al., 2010].

Ideally, climate model ensembles for probabilistic impact studies should be designed to sample the full range of uncertainty. However, in practice they are assembled on an opportunity basis and are restricted by limited resources [Kendon et al. 2010]. GCMs are the primary tool for understanding how climate variables will change. However, their scale is rather coarse, and hydrological processes occur on finer scales. Hence, to assess the influence of climate change on river flows, higher resolution data are required. To resolve this scale discrepancy, different downscaling methodologies have been developed ranging from statistical techniques to the use of RCMs (see Fowler et al. [2007], Haylock et al. [2006], and Maraun et al. [2010]). For the present study, an ensemble of RCM simulations, specifically resampled for flood analysis, was made available through the RheinBlick 2050 project [Görgen et al., 2010]. The RheinBlick 2050 ensemble includes four GCMs from three climate modelling centres, and six different RCMs. It is assumed that the number of GCMs is determinative for the bandwidth of the ensemble. To assess whether this ensemble size is consistent with the spread in a larger model ensemble, 12 different GCM simulations have been downscaled using a delta-change approach [Lenderink et al., 2007; Prudhomme et al., 2002; Te Linde et al., 2010]. This resulted in the largest GCM ensemble used for flood probability estimation in the Rhine basin to date.

The main aim of this research is to provide a demonstration of a framework for producing probabilistic estimates of flood risk, and to demonstrate how ensembles of climate projections can be constructed and used for this purpose.

The main objectives are:

- To generate long resampled time-series of climate variables and discharge for use in probabilistic flood risk assessments;
- To develop probability density functions of extreme discharge under climate change;
- To develop a rapid inundation model capable of providing the large number of inundation maps needed in probabilistic flood risk assessments, and to couple this with a flood damage model;
- To demonstrate the production of flood risk estimates in a probabilistic framework.

This report is set up as follows. In Section 2 we describe the study area, followed in Section 3 with methods and data used in the project. Section 4 describes the results of a pilot study carried out to develop and validate the new inundation model; the pilot study was carried out for the Meuse River in Dutch Limburg, since relatively good data are available for model testing and validation. In this section we also present a limited validation for the Rhine basin. In Section 5 we present the results of the probabilistic flood risk analyses for two case-study stretches of the Rhine in Germany, namely: Bonn-Duisburg; and Mainz-Koblenz. In Section 6 we discuss the findings, limitations, and future research needs, and finally we provide conclusions in Section 7.

2. Study area

The research on probabilistic flood risk assessment focuses on two case-study stretches of the Rhine River in Germany, namely the sections: (a) Bonn-Duisburg; and (b) Mainz-Koblenz (Figure 2.1). However, the climate model downscaling and hydrological modelling were carried out for the entire Rhine River upstream from Lobith (at the German-Dutch border) to produce the relevant input data for future basin-wide studies.

The Rhine originates in the Swiss Alps as a mountain river, fed by glacier water, snowmelt, and rainfall. From Switzerland it flows through Germany, and the Netherlands into the North Sea. The basin has a total catchment area of about 185,000 km^2 with a length of 1320 km, making it the longest river in Western Europe. The annual mean discharge (1901-2000) at Lobith is 2200 m^{3}s^{-1}. The Rhine is one of the most important industrial transport routes in the world [Jonkeren, 2009], and about 58 million people inhabit the river basin, of which an estimated 10.5 million live in flood-prone areas [ICPR, 2001]. In Germany, safety-levels of flood defences vary from a return period of 200 to 500 years; in the two case-study stretches discussed in this report, the return period is 200 years.

Many studies have assessed how climate change may alter the discharge regime of sections of the River Rhine [e.g. Bronstert et al., 2002; Kwadijk, 1993; Kwadijk and Middelkoop, 1994; Lenderink et al., 2007; Menzel et al., 2006; Middelkoop et al., 2001; Shabalova et al., 2003; Te Linde et al., 2010]. However, only recently has an international study assessed changes in the discharge regime over the entire Rhine basin [Görgen et al., 2010]. Using a range of climate change scenarios and modelling methods, these studies suggest that mean winter discharge at Lobith (border Germany-Netherlands; Figure 2.1) may increase by 0 to 30% by 2050, while mean summer discharge may change by -45 to +15%. Moreover, the magnitude of extreme flood events is generally projected to increase. Note that important challenges remain due to large uncertainties in the climate models used as well as the robustness of the hydrological models under changing regimes.

For the Rhine basin, the assessment of current and future flood risk is still in its early phases. The International Commission for the Protection of the Rhine (ICPR) uses the Rhine Atlas approach to estimate aggregated flood damage for the whole basin [e.g. ICPR, 2001, 2005], but: (a) it yields rather low damage potential values for different land use classes compared to other studies [De Moel and Aerts, 2011; Thieken et al., 2008]; and (b) Rhine Atlas does not differentiate between different urban classes, whilst such a differentiation is essential for flood damage estimates [Apel et al., 2009]. Recently, Te Linde et al. [2011] estimated flood risk along the River Rhine using the Damagescanner model [Klijn et al., 2007; Aerts et al., 2008], but only assessed the damage for one return-period, and did not carry out a probabilistic risk analysis. As mentioned in the introduction, Apel et al. [2006] developed a simple stochastic approach for probabilistic risk estimates in a section of the Rhine between Cologne and Rees, with a focus on the polder at Mehrum.
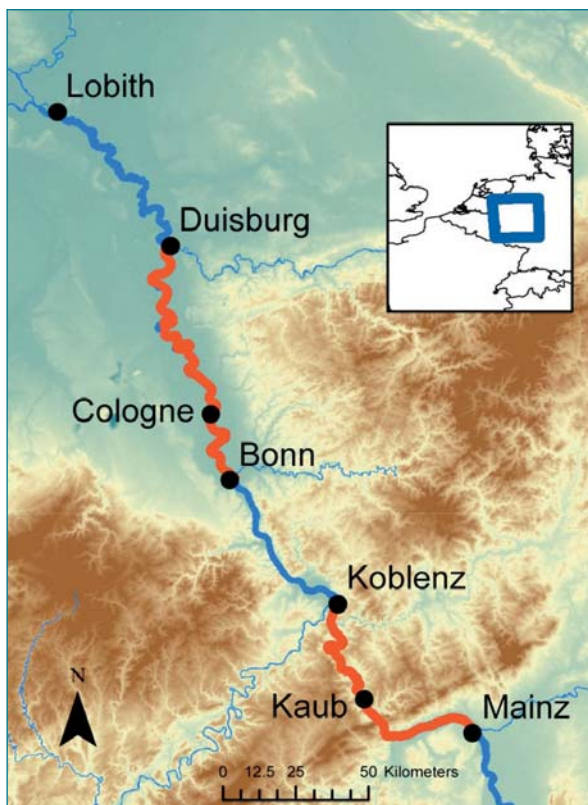

Figure 2.1.
Map of the two case study sections (in red) of the River Rhine.

3. Methods

In this section we discuss the data and methods used in the study. In essence, the overall approach can be broken down into the following steps:

- Generating long (3000-year) climate time-series;
- Generating long (3000-year) discharge time-series;
- Estimating discharge values for low probability flood events;
- Simulating flood inundation extent and depths;
- Estimating flood damage;
- Estimating flood risk and probability distributions of flood risk.

In the rest of this section we describe each of the methodological steps in detail.

3.1 Generating long (3000-year) climate time-series

For this research, bias-corrected, resampled time-series of 3000 years from an ensemble of six RCM simulations were made available through the RheinBlick 2050 project [Görgen et al. 2010]. Five of these simulations were carried out in the framework of the EU ENSEMBLES project [Van der Linden and Mitchell 2009]. Some of these RCM simulations were nested in different versions or runs of the same GCM. In order to enlarge the number of GCMs in our ensemble, 12 GCM simulations run in the context of the 3rd Coupled Model Intercomparison Project (CMIP3) were downscaled using an advanced delta-change approach. The models used are listed in the results table, Table 5.1. For this study, a delta-change approach was considered preferable to a dynamical downscaling technique since the latter is computationally intensive. Downscaling with the delta-change approach on the other hand is comparatively cheap and is able to incorporate observations into the method. We used an advanced method to account for the changes in extreme rainfall and temperature variability, and not just changes in the mean (see Section 3.1.1). Note that the potential evapotranspiration is calculated based on temperature within the hydrological model (Section 3.2).

The GCM simulations used were all driven by the Intergovernmental Panel on Climate Change (IPCC) Special Report on Emission Scenarios (SRES) A1B emission scenario. Since the aim of this project is to demonstrate methods and framework that can be used in probabilistic flood risk assessment, we only used one scenario for demonstrative purposes; of the IPCC SRES scenarios the A1B scenario has the most model runs available. We selected daily data from the GCMs for a control period of 35 years (1961-1995) and a future period of 20 years (2081-2100). Observations of precipitation and temperature from the International Commission for the Hydrology of the Rhine basin (CHR) were used, which contain area-averaged daily precipitation and temperature for 134 sub-basins of the Rhine, for the period 1961-1995. These short (35-year) time-series were resampled to produce long (3000-year) time-series. An advanced delta method was applied to transform the resampled data for each of the 134 sub-basins of the HBV-96 hydrological model in accordance with the changes in the GCM output. The transformation is discussed first in Section 3.1.1, and the time-series resampling is described in Section 3.1.2.

3.1.1 Delta-change approach

Applying a delta method essentially involves transforming observed data such that the changes correspond to those derived from the GCM control and future run. The main points of the delta method used in this study are presented below [see also Van Pelt et al., 2011a; 2011b; in prep.].

3.1.1.1 Precipitation

Firstly, non-overlapping observed 5-day average precipitation amounts over the GCM grid-cells were transformed, using the non-linear formula introduced by Leander and Buishand [2007]:

$$P* = aP^b \qquad (1)$$

where, a and b are empirically derived coefficients to scale the observed precipitation (P) to a future precipitation (P*). Change factors were then applied to disaggregate the transformed 5-day precipitation over the GCM grid-cell to daily values over the 134 HBV-96 sub-basins. An overview of the transformation process can be found in Figure 3.1. The coefficients a and b in equation (1) are derived from the 60% quantile (P_{60}) and the 95% quantile (P_{95}) of the 5-day precipitation sums. Both quantiles are calculated for the control (C) run (1961-1995) and future (F) run (2081-2100) of the GCM precipitation output:

$$a = P_{60}^F/(P_{60}^C)^b * g_1^{1-b} \qquad (2)$$

$$b = \frac{\log\{g_2 * P_{95}^F/(g_1 * P_{60}^F)\}}{\log\{g_2 * P_{95}^C/(g_1 * P_{60}^C)\}} \qquad (3)$$

$$g_1 = P_{60}^O/P_{60}^C \qquad (4)$$

$$g_2 = P_{95}^O/P_{95}^C \qquad (5)$$

The quantities g_1 and g_2 are bias correction factors for the quantiles P_{60} and P_{95}, respectively. The superscript O refers to the observations.

Equation (1) is applied to the observed values for which $P \le P_{95}$. For larger values of P, this equation may result in very high and unrealistic precipitation values, when exponent b is larger than 1. The transformation (1) is also not flexible enough to reproduce changes in the extremes adequately. The latter can be improved by taking into account the change in the mean precipitation of all events > P_{95}, referred to as the excesses $E = P - P_{95}$ of the exceedances of P_{95}. The mean excess for the control and future period is defined as:

$$\overline{E^C} = \frac{\sum E^C}{n^C} \quad \text{and} \quad \overline{E^F} = \frac{\sum E^F}{n^F} \qquad (6)$$

where n^C and n^F are the numbers of 5-day periods during which the 95% quantile is exceeded in the control and future run, respectively. The mean control- and future excess are used to rescale the observations P that exceed P_{95}:

$$P* = \overline{E^F}/\overline{E^C} * (P - P_{95}^O) + a(P_{95}^O)^b \qquad (7)$$
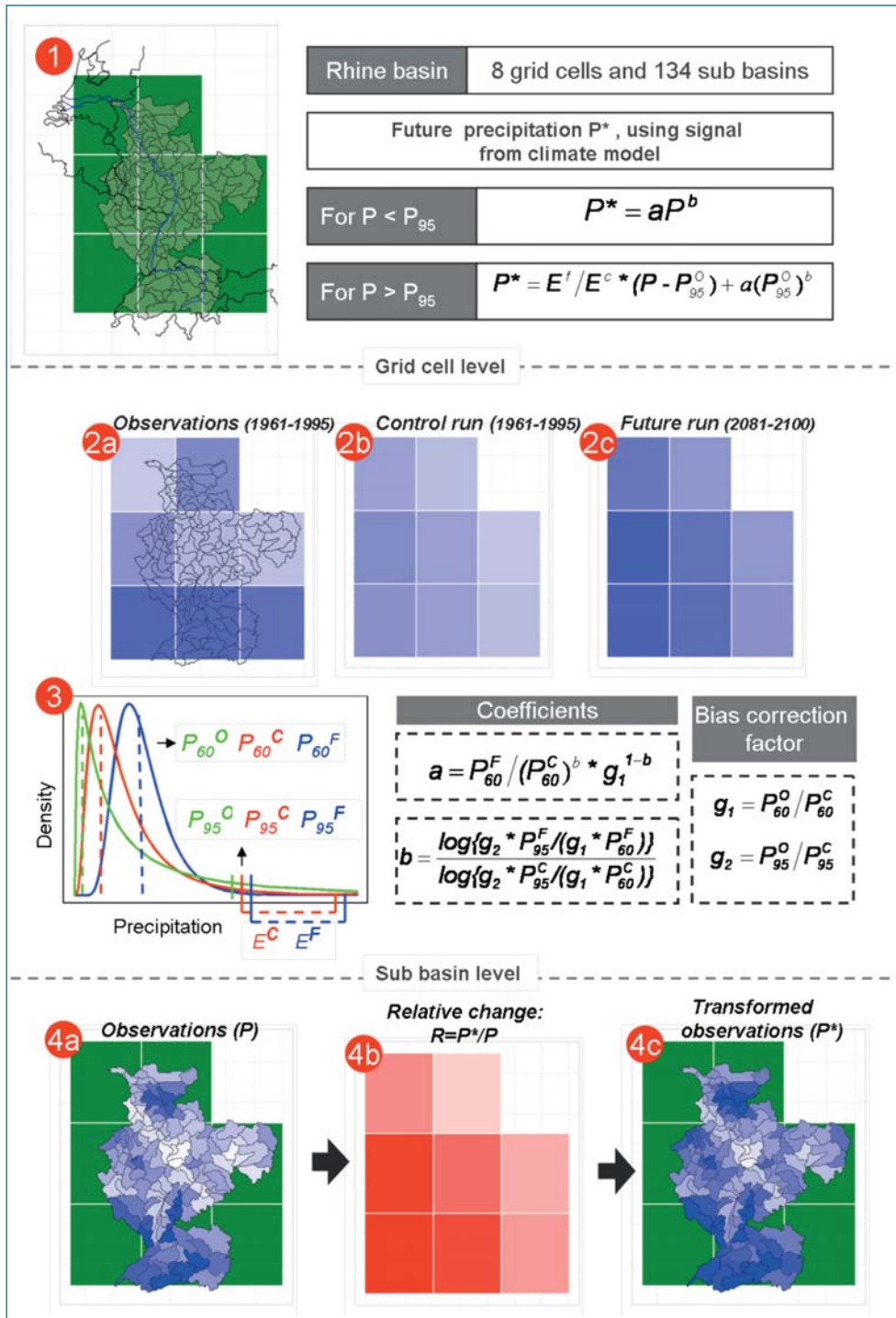
Figure 3.1.
Overview of the climate downscaling methodology. Panel 1 shows the Rhine basin, divided into eight (GCM) grid-cells and 134 sub-basins. Panel 2 shows the mean precipitation over a 5-day period in each grid-cell for the observations and the two GCM runs, all on grid-cell level. The observations are upscaled to grid-cell level by taking a weighted average over the sub-basins. In panel 3 the probability density of 5-day precipitation is shown, with the 60% quantile (P_{60}) and the 95% (P_{95}) quantile (both for the observations and GCM runs). Also the excess, i.e. the amount of precipitation above the 95% quantile, is shown for the control and the future model run. Panel 4 displays the transformation. The daily observations in each sub-basin are multiplied by the change factor R, which is obtained from the observed (P) and transformed ($P*$) 5-day precipitation amount and depends on the coefficients a and b and for $P > P95$ also on E^F/E^C. For each sub-basin the daily precipitation is transformed using the GCM signal from the grid-cell that contains most of its surface area.

The 12 monthly estimates of the quantiles P_{60} and P_{95} are smoothed using a weight of 0.5 on the month of interest and a weight of 0.25 on the previous and next month. Then, equation (3) is applied to obtain monthly estimates of b, and the median of these estimates over the eight grid-cells for each month is taken as the value of b in equations (1) and (7). With these final estimates of b, the values of a are determined using equation (2). The mean excesses E^C and E^F are smoothed both in time in the same way as the quantiles P_{60} and P_{95}, and then the median of their relative changes over the eight grid-cells is taken for each month.

3.1.1.1 Temperature
Observed daily temperature was transformed for each sub-basin taking into account the changes in the mean and standard deviation of the daily temperatures from the GCM simulation:

$$T^* = \frac{\sigma^F}{\sigma^C} * (T - \overline{T^C}) + \overline{T^F}$$

(8)

where $\overline{T^F}, \sigma^F$ are the mean and standard deviation of the future daily temperature series and

$\overline{T^C}, \sigma^C$ are the mean and standard deviation of the control daily temperature series.

3.1.2 Resampling
To estimate extreme quantiles of the distributions of precipitation sums and river discharges, we generated 3000-year synthetic sequences of daily precipitation and temperature by resampling from the historical observations for the 35-year period. These series were then transformed to future time-series with the delta-change approach, as described in Section 3.1.1. The method of time-series resampling of meteorological variables in the Rhine basin was originally developed as part of a new methodology to determine the design discharge for flood protection in the Netherlands [Buishand and Brandsma, 2001; Wójcik et al., 2000]. Nearest-neighbour resampling, as originally proposed by Young [1994], is used to reproduce temporal correlation. Daily precipitation and temperature at different locations in the river basin are sampled simultaneously with replacement from the historical data to preserve their mutual dependencies. The resampling algorithm in this study, which can be regarded as a weather generator, is the same as that used in the RheinBlick 2050 project [Görgen et al., 2010].

3.2 Generating long (3000-year) discharge time-series

The hydrological model used to generate the daily discharge time-series is the HBV-96 model for the Rhine. It is a conceptual model divided into 134 sub-basins for the entire Rhine basin upstream from Lobith, and has a daily time-step. HBV-96 calculates daily potential evapotranspiration by applying a temperature anomaly correction to the long term mean monthly (historical) potential evapotranspiration. The 'robustness' under future climate change of the HBV-96 model is a source of uncertainty as structural changes may occur in the river basin (soil, vegetation, etc.) and empirical parameter values and relations may change in the future. Further details of the applied model can be found in Görgen et al. [2010]. Note that activities are currently being undertaken by Deltares and the German Federal Institute of Hydrology (BfG), in cooperation with the Waterdienst, to re-calibrate the HBV-96 model. The main reasons are to create more transparency in the model's structure, as well as to make use of a newly available climate reference dataset that covers a longer period. It is important to mention that no hydrodynamic modelling was performed, so the effects of upstream flooding on discharge downstream are not considered.

The hydrological model was forced with the 3000-year time-series for the 12 GCM simulations and six RCM simulations described above. The future simulations refer to the period 2081-2100, whilst the reference period is 1961-1995. As described above, the GCM climate time-series were generated by applying the advanced delta-change approach to the resampled CHR dataset (consequently this resampled dataset is the reference time-series for each GCM) whilst the RCM climate time-series were constructed by applying a non-linear bias-correction (based on the CHR dataset) to the resampled RCM data (i.e. each future RCM simulation has its own corresponding control simulation). A validation of discharge computed from the bias-corrected control RCM simulations was applied by comparing discharge values calculated with the CHR data as input by Görgen et al. [2010]. For the middle and lower part of the Rhine basin, which are part of this case study, the extreme discharges from these simulations reproduced observed flood statistics well.

3.3   Estimating discharge values for low probability flood events

The river stretches of the Rhine considered in this study are protected by dikes with a protection level against floods with a return period of approximately 200 years. Hence, we only considered discharge events with a return period in excess of 200 years for the inundation scenarios and damage estimates. As previously described, for each GCM or RCM ensemble member, a 3000-year discharge time-series was generated using HBV-96. From the discharge time-series we took the maximum discharge for each hydrological year (November to October), resulting in 2999 annual discharge maxima per ensemble member. We then estimated extreme discharge using the Weissman approach [Boos, 1984; Weissman, 1978], whereby a joint limiting distribution of the largest order statistics is fitted to the highest 0.5% of the data values. This method provides more consistent results than the Generalized Extreme Value (GEV) distribution fitted to the whole data series [Görgen et al., 2010].

3.4   Simulating flood inundation extent and depths

The methodological framework used in this study requires the simulation of hundreds to thousands of inundation maps showing inundation extent and depth. For detailed flood risk analyses, inundation maps at a high resolution are required from state-of-the-art methods describing the detailed hydrodynamics of the study area [e.g. Ernst et al., 2010]. However, given the large number of simulations needed for our probabilistic framework, we developed a new model, Floodscanner. We used the zero-dimensional planar-based approach, conceptually similar to that described in Priestnall et al. [2000]. The model's setup and development is described in detail in Ward et al. [2011a; 2011b]. The model's performance was first tested and validated for a section of the Meuse River in Dutch Limburg, since relatively good data are available for validation in this river section (e.g. from aerial photography and hydrodynamic modelling using the WAQUA model). This validation, and a validation for the Rhine, are described in Section 4.

Floodscanner is raster-based, with a spatial resolution of 50 m x 50 m. In brief, the method uses stage-discharge relationships to estimate the water level at each river grid-cell within the case-study region, for different discharges. These water levels are then assigned to the nearest non-river grid-cells, essentially creating a planar surface representing the water level per grid-cell. This planar water level is then intersected with a Digital Elevation Model (DEM), and the inundation depth is the difference between the cell values of water level and elevation. Several steps are required to carry out the simulation: (a) derive river network raster; (b) develop stage-discharge relationships; (c) simulate planar water level surface; and (d) estimate flood inundation depth. These steps,

and the data sources used in this study, are described in the following paragraphs. Note that no hydrodynamic modelling was performed, so the effects of upstream flooding on inundation depth downstream are not considered.

a) Derive river network raster: We extracted the river network raster from the SRTM DEM [Jarvis et al., 2006], available from http://srtm.csi.cgiar.org. The DEM has a horizontal resolution of 90 m x 90 m, and was regridded to a higher resolution of 50 m x 50 m. Ideally, a higher resolution DEM would be used, such as a DEM derived from TIN height map used in the WAQUA model of the Rhine basin. Unfortunately, these data were not available for use in this study.

b) Develop stage-discharge relationships: Stage-discharge (*h-Q*) relationships show the relationship between river stage (*h*) at a given point and discharge (*Q*) at that or another point; they can either be observed or derived from models. For a review on the use of *h-Q* relationships, the reader is referred to Braca [2008]. For this study we used relationships derived from the SOBEK model described by Te Linde et al. [2010; 2011]. The data from SOBEK show the river stage corresponding to 30 discharge values. These data are available at irregular distances along the river, but ranging from ca. 0.5 km to 1.0 km. Floodscanner first assigns these values to the correct river grid-cell in the river network raster, and then estimates values for each intervening river cell through linear interpolation. For each river cell, an *h-Q* relationship is then derived in the form:

$$h = aQ^b \qquad\qquad (9)$$

where *h* is the water level (m.a.s.l. NAP), *Q* is the discharge, and a and b are coefficients empirically derived from the data described above.

c) Simulate planar water level surface: For the two sections studied in this research, i.e. Bonn-Duisburg and Mainz-Koblenz, the discharges at Cologne and Kaub respectively are given to the model as input. The model then estimates the corresponding water level at each river grid-cell based on the *h-Q* relationships. All grid-cells in the study area are assigned to their nearest river grid-cell based on the Euclidean distance. This results in a theoretical planar water-level surface for the entire case study area.

d) Estimate flood inundation depth: The elevation of each grid-cell is subtracted from the planar water level surface, to give a theoretical inundation depth per grid-cell. However, this results in cells being inundated where there is no flow connection with the river. Hence, we removed inundated cells not connected to the river via a flow-path with direct connectivity (in at least one of 8 directions).

3.5 Estimating flood damage

We calculated potential direct economic damage for each inundation scenario using the Damagescanner model [Klijn et al., 2007]. Damagescanner has been described in several studies [e.g. Aerts and Botzen, 2011; Aerts et al., 2008; Bouwer et al., 2009, 2010; Te Linde et al., 2011], so we only provide a brief overview here. Damagescanner needs two inputs: a land use map and an inundation map. The land use map (for the year 2000) is derived from the Landuse scanner model [Hilferink and Rietveld, 1999] for the Rhine described in detail by Te Linde et al. [2011]. The inundation maps were derived from Floodscanner. Damagescanner combines information on land use and inundation depth using depth-damage functions, which estimate the expected damage for a given inundation depth (*x*-axis) and a given land use (different curves) for each grid-cell; the depth-damage functions used by Damagescanner are shown in Figure 3.2.
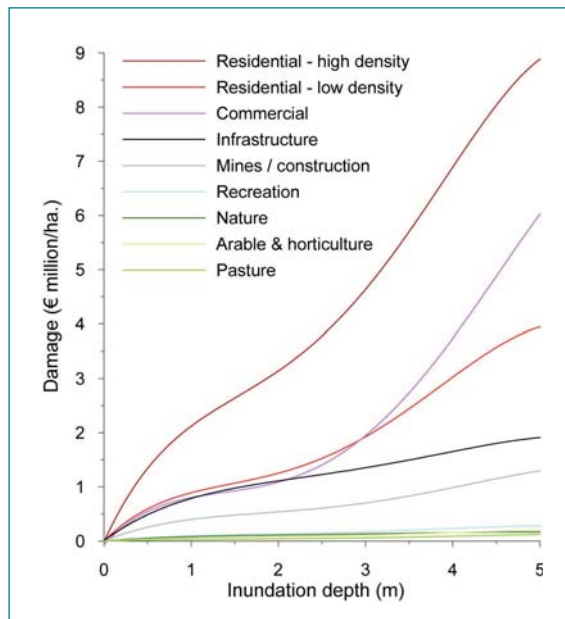
Figure 3.2.
Depth-damage functions used in the Damagescanner model.

3.6 Estimating flood risk and probability distributions of flood risk

Economic flood risk, or expected annual loss, can be considered as the area under an exceedance probability-loss curve (risk curve); a theoretical risk curve is shown in Figure 3.3. In practice, the number of exceedance probabilities used to develop such a curve is limited by available computer and manpower resources; for example in Figure 3.3, loss has been calculated for three exceedance probabilities, and the curve interpolated based on points. However, research carried out as part of this project by Ward et al. [2011a; 2011b] has shown that estimates of flood risk are strongly affected by the choice of exceedance probabilities used to develop the risk curve. We assessed losses associated with return periods between 200 and 3000 years (i.e. exceedance probabilities between 0.005 and 0.00033), with a step of 10 years. A risk curve was developed for the reference climate (resampled CHR-dataset, corresponding to 1961-1995), and also for the future climate for each GCM/RCM ensemble member (corresponding to the late 21st century, ca. 2081-2100). The strict deadlines of the project prevented the development of risk curves for the control RCM time-series to account for remaining biases in extreme events in the RCM ensemble. Risk was calculated for each ensemble member as the area under the risk curve approximated using the trapezoidal rule [e.g. Meyer et al., 2009]. The change in risk between current and future conditions was calculated for each ensemble member in relation to risk estimate for the CHR reference dataset. In a final step, we fitted PDFs to the estimates of risk from each of the climate model simulations, in order to produce the probabilistic risk assessment, and to demonstrate the location of the current risk within this PDF.
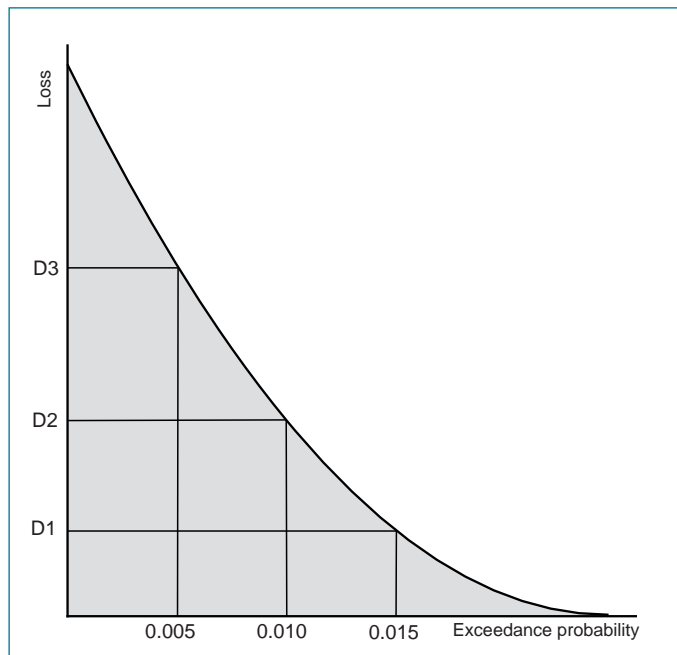
Figure 3.3.
Theoretical exceedance probability-loss (risk) curve; the area under the curve (in grey) represents the risk, expressed as the expected annual loss.

4. Floodscanner: validating the first setup

4.1   Initial setup and validation for the Meuse in Dutch Limburg

As part of this study, and also as part of the Knowledge for Climate study HSGR06, we first setup and validated the Floodscanner approach for the Meuse River in Dutch Limburg. One of the reasons for selecting this area is that relatively good data are available for model validation. The model was then coupled with the existing Damagescanner model. The setup and validation are described in detail in Ward et al. [2011a; 2011b]; these publications also assess how estimates of risk are affected by the selection of return periods (which ones and how many) used to estimate the risk.

Floodscanner was set up for the Meuse basin, following the method described in Section 3.4. However, different data sources were used since this is a different river and case-study area. These are summarised below:

DEM: derived from elevation data used in the WAQUA model of the Meuse (WAQUA-version 2005-02, configuration J09_4). For areas outside the WAQUA configuration we used the AHN5 (Actueel Hoogtebestand Nederland) DEM, which covers the Netherlands at a resolution of 5 m x 5 m. Again, this DEM was regridded to a resolution of 50 m x 50 m.

h-Q relationships: derived from Meuse WAQUA schematisation J09_4, supplied by RWS Limburg.

To verify the quality of the method in producing inundation maps usable in studies of flood damage and risk, we compared: (a) our inundation extent maps with observed inundation extents for the floods of 1993 and 1995; and (b) our inundation depth maps with those produced using the process-based 2D hydrodynamic model WAQUA. These maps were provided by Rijkswaterstaat Limburg (RWS Limburg): Rijkswaterstaat is the executive arm of the Dutch Ministry of Infrastructure and the Environment.

Maps showing the extent of the inundated area during the floods of 1993 and 1995, based on aerial photography and satellite imagery, were provided by RWS Limburg; these floods were associated with discharges at Borgharen of 3120 m^3s^{-1} and 2861 m^3s^{-1} [Wind et al., 1999], corresponding to return periods of ca. 160 and 77 years respectively. Hence, we used these discharge values to force Floodscanner and to derive modelled inundation maps. The observed and modelled flood events were then compared; the results are shown in Figure 4.1.
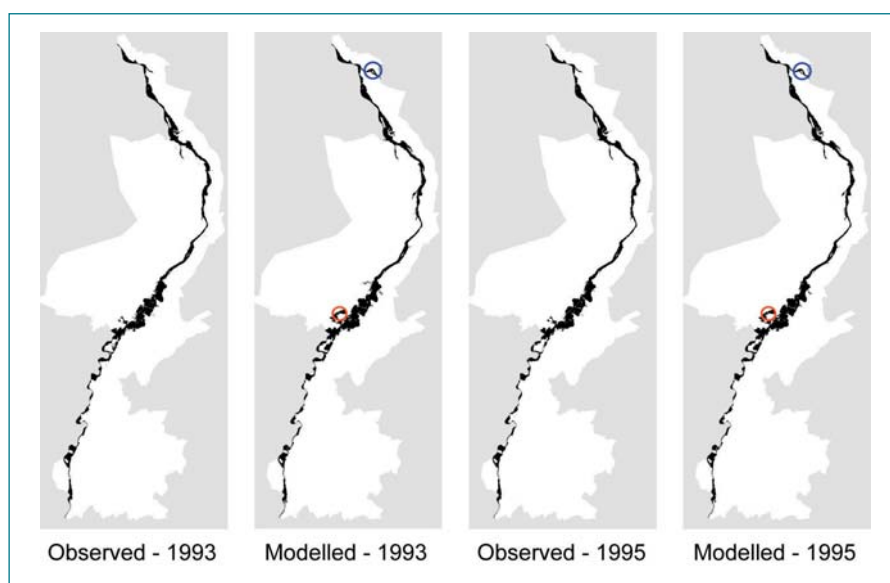
Figure 4.1.
Inundation extent maps based on aerial photography and satellite imagery (observed) and Floodscanner (modelled) for the floods of 1993 and 1995. Blue circles show the confluence of the Niers and Meuse rivers; red circles show the lake known as the Lange Vlieter, completed post-1995.

In Table 4.1 we show the number of cells inundated in the observed datasets only, the modelled datasets only, and the number of cells inundated in both datasets. The agreement between the datasets is good. Reference to the maps (Figure 4.1) shows only a few locations with large differences. For example, the modelled maps show an inundation area at the confluence of the Niers tributary and the Meuse (blue circles). Clearly, the simple inundation model has difficulty in dealing with hydraulically complicated backwater effects. A second source of anomalies is around several of the new 'Maasplassen'; these lakes were created by sand and gravel mining, and some were not completed until after 1995 (e.g. the Lange Vlieter, shown by red circles in Figure 4.2). Hence, these lakes are 'inundated' in our model (which represents the current situation), but were not inundated in 1993 and 1995 because at that time the gravel and sands had not been extracted.

Table 4.1

Number of inundated cells in the observed dataset only, the modelled dataset only, and number of cells that are inundated in both datasets.

	Number of inundated cells		
Year	Observed dataset only	Modelled dataset only	Both datasets
1993	48867	53291	47497
1995	47639	51982	46511

Next, we compared inundation depths per grid-cell for several return periods (2, 5, 20, 75, 250, and 1250 years) between the maps produced using Floodscanner and those produced by WAQUA. The discharge at Borgharen associated with each return period was estimated using the standard formulae provided in the official Dutch *HR2001* guidelines [Van de Langemheen and Berger, 2001]. The depth differences per grid-cell (Floodscanner minus WAQUA) are shown in Figure 4.2. As the return period increases, so too does the spread between the two datasets. The figures show that Floodscanner overestimates inundation depths at very low return periods (2 years), has little bias at medium return periods (up to 20 years) and slightly underestimates inundation depths at high return periods (from 75 years upwards) with respect to the WAQUA estimates. Overall, for the return periods shown, the difference is ≤ 0.5 m for 71% (RP = 1250 years) to 93% (RP = 75 years) of the cells; and the difference is ≤1 m for 91% (RP = 1250 years) to 97% (RP = 10 years) of the cells. Research carried out by De Moel and Aerts [2011] in the Netherlands shows that an overall change in inundation level by 0.5 m (in all grid-cells) may lead to a change in damage by a factor of 1.35-1.44, whilst an overall change in inundation level by 1 m (in all grid-cells) leads to a change in damage by a factor of ca. 2. Hence, Floodscanner performed reasonably well compared to the historical floods of 1993 and 1995, as well as compared to results from a 2D hydrodynamic model (WAQUA).
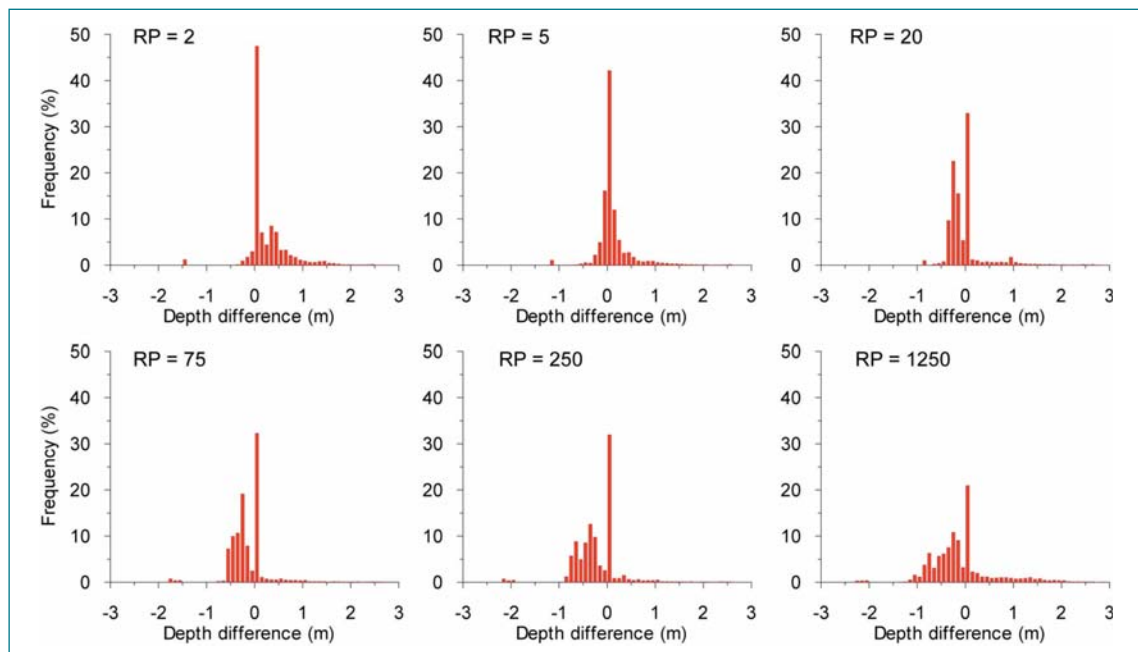
Figure 4.2.

Frequency distributions (%) of the differences between the inundation depth (in metres) per grid-cell in the inundation maps produced using Floodscanner WAQUA (Floodscanner minus WAQUA). The depth differences were only calculated for cells that were inundated in the Floodscanner model (i.e. non-inundated cells are not used in the calculation): the frequency bins have an interval of 10 cm, centred on 0 m.

4.2   Initial validation for the Rhine

A recurring problem in flood risk assessment is the poor availability of high-resolution observed inundation data, making verification difficult (Merz et al. 2010). For the Rhine basin, we were therefore only able to carry out a limited validation. The only publicly available inundation maps of the German Rhine are those developed for the Rhine Atlas (ICPR 2001). This dataset shows the potential flooded area in the Rhine basin at different flood return periods (10 years, 100 years, and 'extreme'). The 'extreme' inundation map, however, does not have a probability estimate; rather it assumes that all potentially flood-prone areas are inundated completely. We compared our simulated inundation depths for a return period of 1250 years with those in the extreme inundation map of the Rhine Atlas. Depth anomalies per grid-cell (Floodscanner minus Rhine Atlas) are shown in Figure 4.3. Overall, the difference is ≤1.0 m for 51% (Bonn-Duisburg) and 41% (Mainz-Koblenz) of the cells. A study by the (Dutch) Ministry of Transport, Public Works and Water Management *et al*. (2004) used the 2D-hydrodynamic model DelftFLS to simulate inundation depths for several scenarios corresponding to a flood return period of 1000 years for the lower Rhine in Germany. Unfortunately, these maps were only made available in paper format; the GIS maps are not available for research activities. However, visual inspection shows the inundation extents in the latter to be much smaller than in the Rhine Atlas. Thus, for this demonstration study of a probabilistic flood framework, our estimates are of sufficient accuracy to give meaningful results.
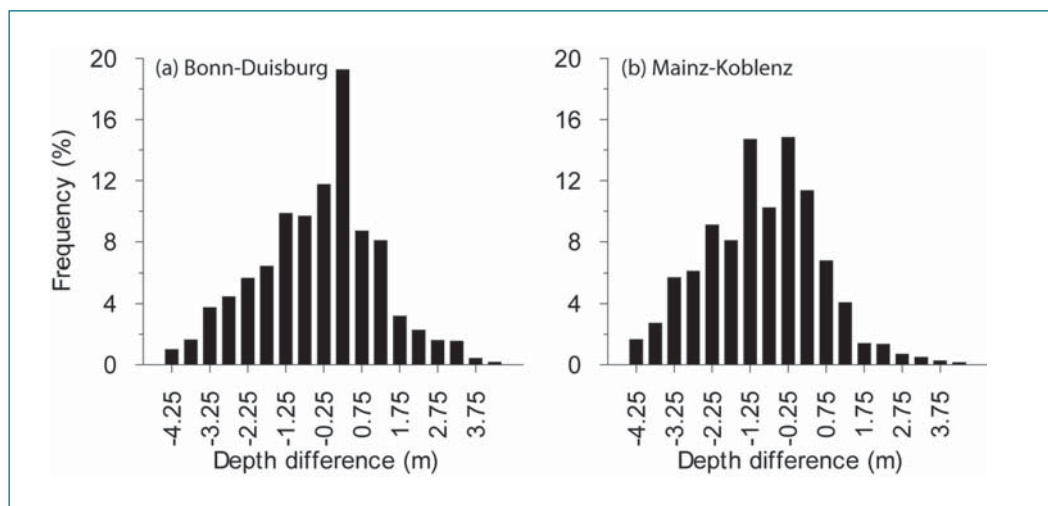

Figure 4.3.
Frequency distributions (%) of the differences between the inundation depth (in metres) per grid-cell in the Floodscanner inundation maps (return period 1250 years) and the Rhine Atlas 'extreme' scenario. The depth differences were only calculated for cells that were inundated in the Floodscanner model (i.e. non-inundated cells are not used in the calculation): the frequency bins have an interval of 25cm, centred on 0 m.

5. Probabilistic flood risk estimates for the Rhine

5.1 Precipitation extremes for GCM simulations

High river discharge and floods in the middle to lower part of the Rhine basin are often associated with multi-day extreme precipitation in the winter season [Beersma et al., 2001]. Therefore, to assess possible future changes in the occurrence of such multi-day extreme precipitation, we compared the winter half-year (Oct-Mar) maximum 10-day precipitation sums of the transformed (resampled) time-series (representative of future conditions in a GCM simulation) with those in the (resampled) observed time-series (Figure 5.1). The figure shows Gumbel plots of the winter half-year maximum 10-day precipitation sums for the short time-series (35-year) (left panel) and for the long time-series (3000-year) based on resampling (right panel). The precipitation is averaged over all sub-basins in the Rhine basin upstream from Lobith. Both panels refer to the largest 10-day precipitation amounts in the winter half-year. Although the spread between the GCMs increases with longer return periods, the range between the GCMs varies between almost no change compared to the reference observations, to an increase of ca. 35 %; this is the case in both the 35-year and 3000-year time-series.
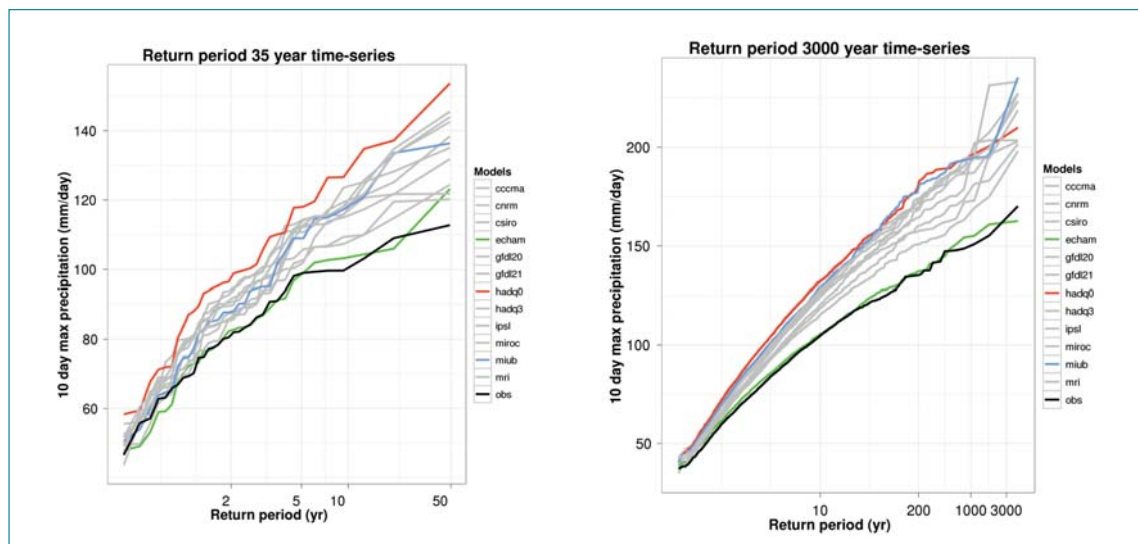
Figure 5.1.
Gumbel plots of winter half-year maximum 10-day basin-average precipitation sums for short time-series of transformed observations (35 years; left) and long time-series of transformed resampled observations (3000 years; right). The black line shows the ordered 10-day maxima in the (resampled) CHR reference dataset; the grey lines represent the individual GCM ensemble members; and the coloured lines denote the GCM ensemble members generating the lowest and highest precipitation sums.

5.2 Range of quantiles of the maximum 10 day precipitation sum for the GCM and RCM ensembles

Figure 5.2 shows the range in the quantiles of the winter half-year maximum 10-day basin-average precipitation sum for different return periods, derived from the RCM and GCM ensembles. For the RCM ensemble, the quantiles for the control and future periods are shown. For the GCM ensemble, the estimated quantiles from the resampled observations are shown as a reference, together with the range of the estimated quantiles for the transformed resampled observations for the future

period. The GCM ensemble shows higher quantiles of winter half-year maximum 10-day basin-average precipitation sums than in the RCM future ensemble for each return period, while the RCM control ensemble is fairly consistent with the observations (due to the bias correction applied to the RCM data). This means that the GCM ensemble shows a larger change in quantiles of extreme precipitation sums compared to the RCM ensemble. The spread within the ensembles is roughly similar, except at short return periods, where the spread of the RCM ensemble is slightly larger.
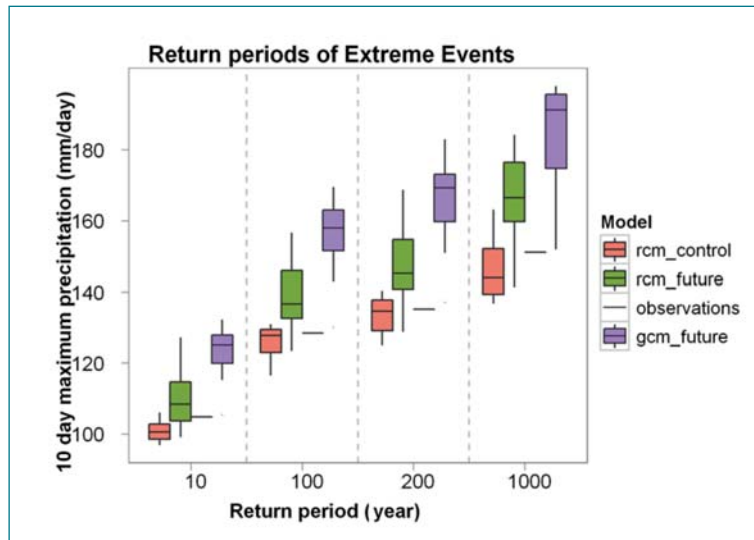

Figure 5.2.
The winter half-year maximum 10-day basin-average precipitation sum for four return periods generated with the RCM and GCM ensembles. Each box-plot contains the median, the 25th and 75th percentiles, and the smallest and largest values (the whiskers) for the given return period for all members of the RCM or GCM ensemble. For the observations there is only one estimate.

5.3   Discharge extremes

In order to assess possible future changes in discharge compared to present day, Figure 5.3 shows the mean annual maximum discharge (MHQ) and the 200- and 1000-year discharges (HQ200 and HQ1000 respectively) at Lobith, Cologne, and Kaub. Also the reference values for the 1961-1995 period are indicated based on the CHR dataset. A thorough analysis of the reference values resulting from the CHR dataset (as well as the control runs of each RCM) is described in Görgen et al. [2010].

In general, the (resampled) time-series indicative of future conditions tend to show an increase in the estimated quantiles of average and extreme discharge compared to the (resampled) CHR reference dataset. These increases are generally greater for the GCM ensemble compared to the RCM ensemble, although the relative difference between the two ensembles is less than that seen for extreme 10-day precipitation sums in Figure 5.2. This indicates a non-linearity in the process of transforming precipitation to discharge.

Still, there are also several ensemble members that do project a decrease in flood discharges (ECHAM GCM, and ARPEGE-HIRHAM5 and ECHAM-REMO 10km RCMs for the 200 and 1000 year return periods at Cologne and Lobith; and the HADCM3Q0-CLM and ECHAM-REMO 10km RCMs for the 1000 year return period at Kaub).
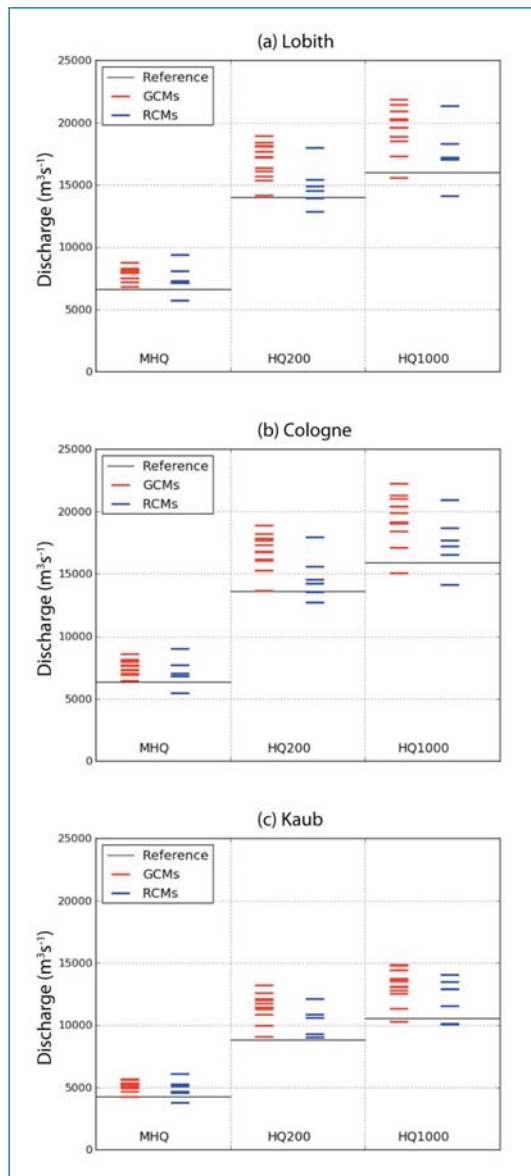
Figure 5.3.

Plots for (a) Lobith, (b) Cologne, and (c) Kaub, of projected: mean annual maximum discharge (MHQ); and 200- and 1000-year discharges (HQ200 and HQ1000). GCM members are shown in red, and RCM members in blue (both representing future conditions). The black lines denote the discharge for the CHR reference dataset (1961-1995). All values based on resampled 3000-year time-series. For MHQ, the bandwidth of the RCM ensemble is larger than that of the GCM ensemble, despite the fact that the latter ensemble contains twice as many members. For HQ200 and HQ1000 the bandwidths are similar at both Lobith and Cologne, as was the case between the ensembles for precipitation. However, the bandwidth of the GCM ensemble is slightly larger than that of the GCM ensemble at Kaub.

At Kaub, the highest HQ1000 is for the MIUB GCM, whereas at Cologne and Lobith the HADCM3Q0 GCM is the highest. The MIUB GCM simulates much wetter conditions in the river basin upstream from Kaub, whilst the HADCM3Q0 GCM simulates the wettest conditions in the lower part of the basin and the Mosel river basin. It is noteworthy that whilst the HADCM3Q0 GCM simulates very wet conditions, the RCM simulation HADCM3Q0-CLM (i.e. the CLM RCM forced by the HADCM3Q0 GCM) is one of driest simulations. Hence, the RCMs have a large influence on the results of the climate projections.

5.4 Meteorological indicators of extreme discharge

Previous analyses by Leander et al. [2008] for the Meuse have shown that changes in the distribution of extreme discharges strongly depend on changes in average winter half-year precipitation and the coefficient of variation of 10-day precipitation in the winter half-year. This suggests a relationship between changes in the quantiles of extreme discharge and changes in the corresponding quantiles of the winter half-year maximum 10-day precipitation sum. In Figure 5.4 we test this relationship for the Rhine basin, by plotting the relative changes in discharge at Lobith with a return period of 200

years versus relative changes in the winter half-year maximum 10-day basin-averaged precipitation sum with a return period of 200 years. Each point in the graph represents one ensemble member of either the RCM ensemble (blue) or the GCM ensemble (red). The same analysis was applied for 10 and 1000 year return periods, and different seasonal definitions, but the results were similar. The winter half-year maximum 10-day precipitation sum is shown to be a fairly accurate predictor of changes in the peak discharge regime. Including temperature of the Alpine grids (indicative of snow melt) in the analysis did not lead to improved predictions of the changes in extreme discharges.
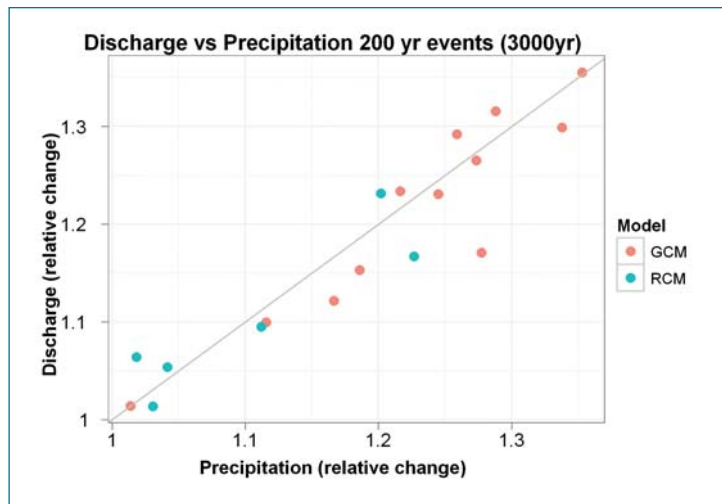
Figure 5.4.
Relative change in the 200-year discharge at Lobith compared to the relative change in the 200-year 10-day basin-average precipitation. Each symbol represents one GCM or RCM (red: GCMs, blue: RCMs).

5.5 Extreme discharge probability distributions

So far we have presented the results of the individual members of the RCM and GCM ensembles. However, one of the main aims of this research is to provide a demonstration of a framework for producing probabilistic estimates of flood risk. Before assessing the risk in a probabilistic framework, we first present PDFs of the extreme discharge results. Figure 5.5 shows PDFs for the RCM and GCM ensembles, based on the normal distribution (for Lobith, Cologne, and Kaub). The normal distribution does not necessarily give the best fit to the data, but considering the low number of ensemble members it is used as a demonstration of how probabilistic assessments of flood scenarios can be developed. In this case the PDFs are given for discharge with a return period of 1000 years (HQ1000). The HQ1000 for the CHR reference dataset is shown by the black line. The GCM ensemble is based on transformed resampled CHR data conform to the changes in the GCM simulations; the RCM ensemble is based on the individual future RCM ensemble members.
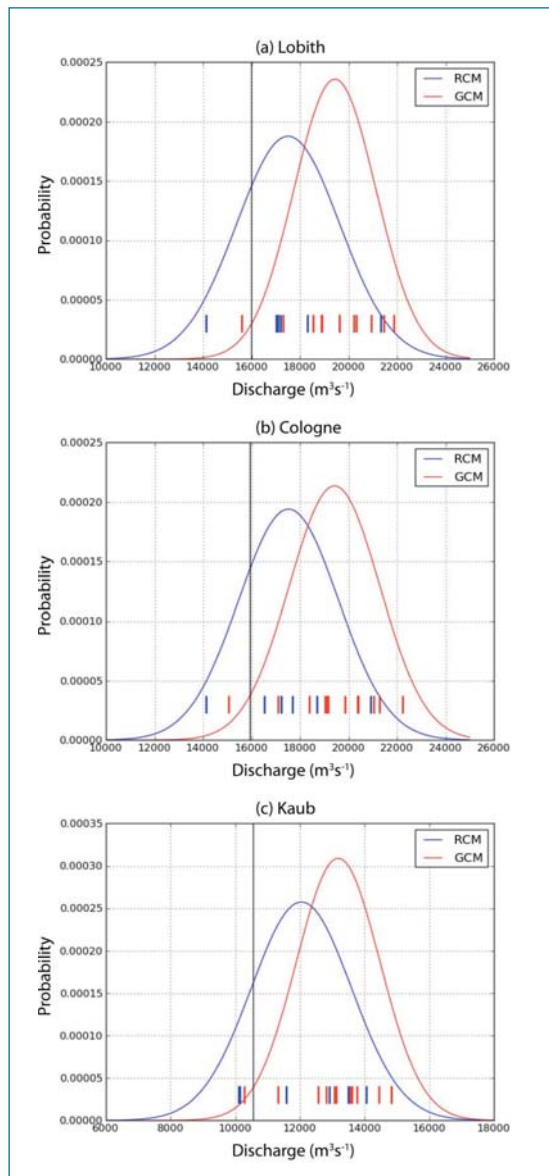
Figure 5.5.
PDFs of HQ1000 at: (a) Lobith, (b) Cologne, and (c) Kaub. As the number of ensemble members is limited the normal distribution used is only demonstrative. The black line shows the 1000 year flow for the resampled CHR reference dataset (as resulting from our hydrological simulations) for current climate conditions.

5.6 From extreme discharge to risk

The next step in our research was to derive flood risk estimates based on the climate model downscaling and hydrological simulations. As described in Section 3.6, the risk was estimated as the area under an exceedance probability-loss curve, using the trapezoidal rule. A risk curve was developed for each (future) RCM and GCM ensemble member and for the CHR reference dataset, using damage estimates with return periods between 200 and 3000 years (i.e. exceedance probabilities between 0.005 and 0.00033), with a step of 10 years. We assumed that no damage occurs at flood return periods shorter than 200 years, due to safety measures designed for this return period. We also estimated the risk by simply summing the modelled damage associated with the top-15 discharge events per ensemble member (i.e. those with a return period of 200 years or longer), and dividing this by 3000 (years); this led to very similar results. Hence, the results shown in this section are those obtained by estimating the area under the risk curve.

The risk curves for each ensemble member (RCMs in blue; GCMs in red) and for the CHR reference dataset (black solid line) are shown in Figure 5.6. Again, the GCM ensemble is based on transformed resampled CHR data for each GCM simulation; the RCM ensemble is based on the individual future RCM ensemble members. In Table 5.1, several key statistics referring to each ensemble (RCM, GCM, full ensemble) are listed. The range between the maximum and minimum risk estimate is slightly larger in the GCM ensemble than in the RCM ensemble for both case-study areas, although the standard deviation is smaller. However, the differences between both ensembles are small and may be partly related to the difference in ensemble size. Nevertheless, the mean risk is higher for the GCM ensemble compared to the RCM ensemble for both the sections Bonn-Duisburg and Mainz-Koblenz.
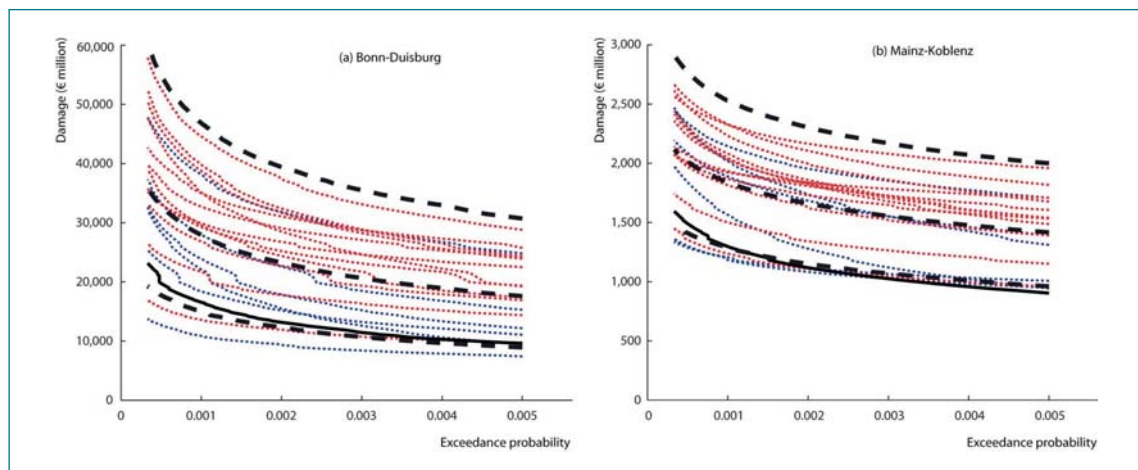
Figure 5.6.
Risk curves for Bonn-Duisburg (left) and Mainz-Koblenz (right). The solid black line shows the risk curve for the CHR reference dataset. Risk curves for the future RCM ensemble members are shown in blue, and for the future GCM ensemble members are shown in red. The black dashed lines show the average and the 5% and 95% percentiles of a two-parameter gamma distribution fitted to all members of the full future model ensemble.

Table 5.1.
Key statistics related to the (future) annual risk (€ million) for the two case-study regions for the RCM ensemble, the GCM ensemble, and the full ensemble. For comparison, risk for the reference simulation is € 60.3 million for Bonn-Duisburg and € 5.1 million for Mainz-Koblenz.

	Bonn-Duisburg			Mainz-Koblenz		
	RCM ensemble	GCM ensemble	Full ensemble	RCM ensemble	GCM ensemble	Full ensemble
Maximum	145.9	170.4	170.4	9.0	10.0	10.0
Minimum	42.6	54.2	42.6	5.0	5.1	5.0
Range	103.3	116.2	127.7	4.0	4.9	5.0
Mean	85.1	121.0	109.1	6.7	8.1	7.7
St. dev.	35.1	31.6	36.3	1.7	1.4	1.6

The results are shown for each ensemble member in Table 5.2. Next to total annual risk (based on damage to all land use categories), we also show risk per capita for residential losses only (residential risk per capita). To do this, we calculated the expected annual loss (risk) based only on the damage estimates for residential grid cells (high and low density). We then divided this by the number of people living in the area exposed to the 3000-year return period flood. The latter was estimated

using LandScan2008™ data [LandScan, 2008]. Such information could be of use when calculating insurance premiums for private households. Interestingly, whilst the total annual risk is higher for the section Bonn-Duisburg – since the inundation extent in this area is much larger and the area is more urbanised – the annual residential risk per capita in the former is lower.

The highest risk is simulated for Bonn-Duisburg by the HADCM3Q0 GCM, and for Mainz-Koblenz by the MIUB GCM. This is consistent with the extreme discharge results (HQ1000), for which these models resulted in the highest values at Cologne and Kaub respectively. The lowest risk is simulated by the ECHAM5R1-REMO RCM and the HADCM3Q0-CLM RCM for Bonn-Duisburg and Mainz-Koblenz respectively.

5.7   Probabilistic flood risk estimates

The final step in the analyses is the presentation of a probabilistic scenario of future flood risk, demonstrating how this approach could be further developed in the future as more and more tailor-made probabilistic climate change scenarios become available. The probabilistic future flood scenario consists of a PDF of future risk, based on the individual ensemble members. We applied a two-parameter gamma distribution to the individual risk estimates within each future ensemble (RCM, GCM, and full ensemble), whereby each ensemble member was assumed to have an equal likeliness (i.e. no weighting was carried out). We assumed a two-parameter gamma distribution, since this is left-bounded to zero (i.e. no negative risk can be predicted) and is frequently used in risk analysis. The resulting probabilistic flood risk scenarios can be found in Figure 5.7, and the average and 5% and 95% percentiles of the gamma distribution are also shown on the risk curves in Figure 5.6.

Figure 5.7 shows that the addition of the GCM ensemble to the existing RCM ensemble from RheinBlick 2050 leads to an increase in the spread of the PDF, and also leads to a higher mean estimate of flood risk. For the section Bonn-Duisburg, two ensemble members of the full ensemble fall below the 5% percentile of the distribution (ECHAM5R1-REMO; ECHAM5). For the section Mainz-Koblenz, three ensemble members of the full ensemble fall below the 5% percentile of the distribution (HADCM3Q0-CLM; ECHAM5R1-REMO; ECHAM5).

Table 5.2.
Annual risk and annual residential risk per capita for the two case-study regions.

Climate simulation	Bonn-Duisburg		Mainz-Koblenz	
	Annual risk (€)	Annual residential risk per capita (€)	Annual risk (€)	Annual residential risk per capita (€)
Reference (1961-1995)	60,276,307	24	5,132,916	44
RCMs				
ARPEGE; HIRHAM5	70,882,826	28	5,809,432	50
ECHAM5R1; REMO	42,617,043	16	5,138,936	44
ECHAM5R3; RACMO	145,876,835	61	9,002,613	79
ECHAM5R3; REMO	99,833,127	41	7,658,706	66
HADCM3Q0; CLM	69,300,307	27	4,988,060	42
HADCM3Q3; HADRM3Q3	82,156,253	33	7,817,551	68
GCMs				
CCCMA	114,928,051	47	8,305,417	73
CNRM	121,894,832	50	8,352,761	73
CSIRO	82,212,647	33	6,194,293	53
ECHAM5	54,179,309	21	5,111,187	44
GFDL 2.0	100,975,776	41	7,466,638	65
GFDL 2.1	148,693,686	63	9,145,282	80
HADCM3Q0	170,362,813	73	9,658,859	85
HADCM3Q3	133,293,053	56	8,489,891	74
IPSL	128,905,749	54	8,269,451	72
MIROC	109,325,301	45	7,937,314	69
MIUB	142,785,242	60	10,001,199	88
MRI	144,939,789	61	8,465,437	74
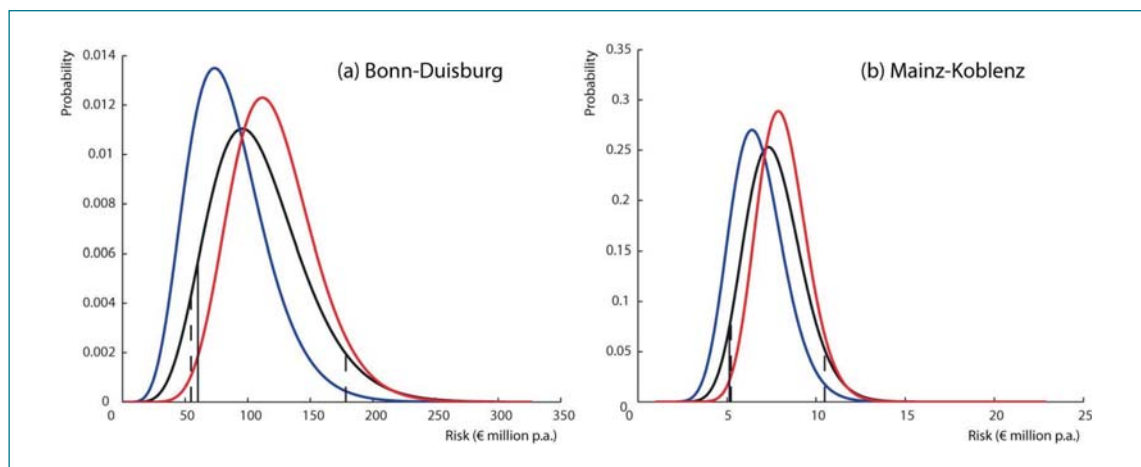
Figure 5.7.
Probability distribution of flood risk for: (a) Bonn-Duisburg (left); and (b) Mainz-Koblenz (right). The black vertical solid line shows risk associated with current climate conditions (based on the resampled CHR reference dataset (1961-1995)). Curves show the risk probabilities derived from the RCM ensemble (blue), GCM ensemble (red), and full ensemble (i.e. all members of the RCM and GCM ensembles). Distributions are obtained by applying a two-parameter gamma distribution.

6. Discussion

6.1 Developing long time-series of climate variables and discharge for use in probabilistic flood risk assessments

Long time-series (3000-year) of daily climate variables (precipitation and temperature) and discharge were developed based on 12 GCMs and six RCMs. The time-series for the RCM simulations were made available through the RheinBlick 2050 project [Görgen et al., 2010], while the GCM simulations were downscaled with an advanced delta-change approach. The winter half-year maximum 10-day basin-average precipitation sums were analysed, as these events often cause high discharge in the lower part of the Rhine basin [Beersma et al., 2001]. The range between the 12 GCM ensemble members representing future conditions was about 35% for the longest return period studied (3000 years). Moreover, the GCM ensemble showed higher quantiles of winter half-year maximum 10-day precipitation sums than in the RCM future ensemble for each return period. The analyses also show that the bias-corrected RCM control time-series match the CHR reference dataset fairly well. The spread between the estimated quantiles of the winter half-year maximum 10-day precipitation sums for the RCM future ensemble members increases as the return periods become longer.

For the extreme discharge events, the bandwidths of the two ensembles are similar at Lobith and Cologne, but the bandwidth of the RCM ensemble is slightly smaller than that of the GCM ensemble at Kaub. We also found interesting spatial differences in the results. For example, the climate model ensemble members do not cause the same changes in extreme discharge in all parts of the basin. This demonstrates the importance of using spatially distributed climate simulations when carrying out climate change impact studies.

The results show that adding the ensemble of 12 GCM members to the existing ensemble of six RCM members (driven by four parent GCMs) from RheinBlick 2050 leads to a relatively small increase in the overall spread of the extreme discharge results, although the ensemble means of the estimated discharge quantiles are higher for the GCM ensemble (as was the case for extreme precipitation). Given the large range of GCMs, one may have expected a larger increase in the spread when they were added to the RCM ensemble. The ensemble of RCM members used for the extreme discharge analyses was selected from a total of 17 members used in the RheinBlick 2050 study. These 17 ensemble members include combinations of four GCMs and 11 RCMs. Hence, even if the RCM ensemble members used for the extreme analyses (i.e. the RCM members used here) were chosen in an optimal way, the number of parent GCMs is still much lower than the 12 GCMs used in the present study. It appears that the RCMs used in this project have a large influence on the climate, and therefore discharge, projections. This is demonstrated by the fact that whilst the RCM ensemble member HADCM3Q0-CLM (i.e. the CLM RCM forced by the HADCM3Q0 GCM) is one of driest members, the HADCM3Q0 GCM ensemble member (not coupled to an RCM) is the wettest.

6.2 Relationship between variables of extreme climate and discharge

The relative change in the winter half-year maximum 10-day basin-average precipitation was found to be a relatively good predictor of extreme discharge. However, in the analyses, extreme precipitation and discharge values were determined independently, so the annual maxima of the precipitation and discharge events may have been related to different episodes or events.

In reality, the relationship between precipitation and discharge is complex [Ward and Robinson, 1990], especially for a large river basin such as the Rhine. In some basins, temperature (through its influence on potential evapotranspiration) can play an important role in this relationship [Ward et al., 2011c]. For the Rhine basin, temperature also plays an important role in snow accumulation and snowmelt, which can significantly affect the river's discharge [Hurkmans et al., 2010; Te Linde et al., 2010]. However, additional analyses carried out for this research (not shown) did not result in a stronger relationship between predicted extreme precipitation and discharge when temperature was included. Other factors may also be of influence in the relationship between extreme precipitation and discharge, such as soil moisture, groundwater levels, infiltration rates, flow routing, land cover, and land use [e.g. Ward and Robinson, 1990].

Nevertheless, the results presented here do suggest that, for the Rhine basin, multiday precipitation can give a first estimate of effects of changes in the discharge regime, although they cannot replace the complex behaviour of the non-linear and heterogeneous hydrological system. Also, hydrological models used for large scale river basins like the Rhine are conceptual and calibrated towards the current climate, resulting in a limited robustness under climate change. Both of these areas, i.e. the use of multiday precipitation totals as a first-order estimator of discharge, and improving the 'climate change robustness' of hydrological models, warrant further research.

6.3 Developing an inundation model capable of providing the large number of inundation maps needed in probabilistic flood risk assessments

One of the main problems in developing probabilistic flood risk assessment methods has been the large number of inundation maps required, since the production of flood hazard maps is very time-consuming and computationally expensive [Apel et al., 2008; Gouldby and Kingston, 2007; Woodhead et al., 2007]. Therefore, in this project we developed a rapid flood inundation model (Floodscanner), and coupled it to an existing flood damage model (Damagescanner).

For the Rhine basin, relatively few inundation maps are available for model validation. Hence, we first setup the model for a section of the neighbouring Meuse basin in Dutch Limburg. Floodscanner performed reasonably well compared to images of the historical floods of 1993 and 1995, as well as compared to results from a process-based 2D hydrodynamic model (WAQUA) [Ward et al., 2011a; 2011b]. We also carried out a limited validation for the Rhine basin [Ward et al., 2011d, in prep.], by comparison of the flood extents simulated by Floodscanner with those in the Rhine Atlas [ICPR, 2001].

The simplifications used in the approach do not allow flood damage estimates at fine resolutions (e.g. street to city scale), which need state-of-the-art hydraulic modelling methods [e.g. Ernst et al., 2010]. Rather, the approach is intended to be complementary to such methods for use in regional-to-basin scale studies in which large numbers of inundation maps are required. For example, where accurate basin-wide flood risk estimates are required, it may be useful to first employ a method such as Floodscanner to identify the sensitivity of the risk estimates to the number of return periods used to develop the risk curve. Once these have been established, it may still be preferential to employ a more complex process-based model to simulate inundation for a selected number of return-periods [Ward et al., 2011a, 2011b].

In addition, the coupled methodology is useful for Monte Carlo based uncertainty analyses [e.g. Apel et al, 2008] and the evaluation of combinations of many different future projections. In the latter case, Floodscanner can be used to derive change factors for many different future projections, which

can then be applied to detailed baseline estimates of risk under current conditions using damage estimates based on the most state-of-the-art process models. As illustrated, there are many cases where large numbers of model evaluations are useful. This shows that more attention is needed on the development of relatively simple inundation models. The method developed and applied here is capable of this, but refinements could be added to include the most important physical processes in a simple manner.

6.4   Flood risk estimates in a probabilistic framework

The present research is the first attempt to assess future flood risk under climate change in a probabilistic framework. It should be understood as a first demonstration of the methodological steps needed to perform such an assessment. In this research, the size of the full ensemble used to develop the PDFs of risk (18 members) is still fairly limited. This means that the selection of a theoretical distribution to describe the PDF of risk is also difficult [e.g. Hall, 2007; Hall et al., 2007; New et al., 2007; Rougier, 2007]. In this study we assumed a two-parameter gamma distribution, since this is left-bounded to zero (i.e. no negative risk can be predicted) and is frequently used in risk analysis. We did not assign weights to individual model members. Theoretically, a weighting could be given to each GCM/RCM simulation based on its ability to realistically downscale observed climate for the reference period. However, models that reproduce the past climate are not necessarily those that will give the most realistic realisation of future climate.

Keeping these limitations in mind, the results do demonstrate the potential use of the approach, especially given the ongoing research efforts in developing probabilistic climate change projections for the Fifth Assessment Report (AR5) of the IPCC. For example, a novelty of the probabilistic risk assessment approach is that it allows us to estimate the probability of future flood risk being larger than present flood risk. Based on the analyses in this study, the probability of future flood risk exceeding current risk is 92% for the section Bonn-Duisburg and 96% for the section Mainz-Mosel. Moreover, the probability of future flood risk exceeding twice as much as at present is 34% for Bonn-Duisburg, but just 6% for Mainz-Mosel. By extension, it is possible to assess the probability that flood risk will increase by any given factor, allowing for the assessment of risk under possible extreme futures. Figure 5.7 shows that the addition of the GCM ensemble to the existing RCM ensemble from RheinBlick 2050 leads to an increase in the spread of the PDF, and a higher mean estimate of flood risk.

A recent study by Te Linde et al. [2011] examined flood risk for the entire Rhine basin, for a reference year 2000 and two climate change scenarios for 2030. The scenarios were derived using different methodologies [Te Linde et al, 2010] and are labelled as "extreme" and "moderate". The "extreme" scenario represents an extreme climate change scenario corresponding to a 2°C increase in global temperature in 2050 with respect to 1990, and changes in atmospheric circulation resulting in drier summers and wetter winters in the Netherlands. This scenario is based on the so-called KNMI'06 W+ scenario of Van den Hurk et al. [2006, 2007]. The "moderate" scenario represents more moderate climate change effects, and follows the output of the RACMO2.1 RCM driven by the ECHAM5 GCM. As with the climate model runs used in the present study, this run corresponds with the IPCC SRES A1B scenario. Te Linde et al. [2011] simulated increases in basin-wide flood risk of 43% (moderate) and 161% (extreme) by 2030 (compared to 2000). Results from our demonstration study suggest that the probability of flood risk increasing by 43% by 2081-2100 is 67% for Bonn-Duisburg and 55% for Mainz-Koblenz, whilst the probability of flood risk increasing by 161% by 2081-2100 is 11% for Bonn-Duisburg and 0.1% for Mainz-Koblenz. A comparison with results of Te Linde et al. [2011] is limited by: (a) the use of different methods to calculate risk; (b) the choice of a different analysis period; and

(c) a different areal aggregation level. However, these limitations notwithstanding, the extreme risk estimate of Te Linde et al. (2011) is at the upper tail of our results. This comparison illustrates an interesting feature of the probabilistic framework explored here: it allows evaluation of a discrete scenario in the context of a wider probability distribution.

Such probabilistic information could provide information of use to stakeholders in the insurance industry. For example, it could aid insurers and reinsurance companies in computing insurance premiums under uncertainty [Michel-Kerjan, 2008] and deriving the amounts of capital reserves required for potential damage reimbursements. Our results also illustrate how spatially differentiated estimates of risk per capita can be developed. For example, our demonstrative analyses suggest that whilst the total annual risk is higher for the section Bonn-Duisburg than for Mainz-Koblenz, the annual residential risk per capita is lower. Moreover, information about extreme risk is relevant for decisions concerning the hedging of the tails of the loss distribution on reinsurance or capital markets [Froot, 1999]; the tails of the flood risk PDFs could assist in such assessments. At the moment, insurance coverage for flood damage is not available in the Netherlands. In recent years, insurers, the government, as well as academics, have been examining the possibilities of introducing partly private flood insurance [Botzen and van den Bergh, 2008; 2009]. In cases where governments (partly) compensate for the flood damages, like in the Netherlands, the framework can also provide information to the government about its financial risk exposure [Grossi and Kunreuther, 2006].

6.5   Key limitations and recommendations for future study

This project presents the first assessment of future flood risk under scenarios of climate change in a probabilistic framework. It is intended to give a demonstration of the methods that can be used in such a framework. The absolute figures should be used for qualitative comparison only in decision-making at this time. Of course, there remain several key limitations, and many opportunities for further research; these are listed briefly, and discussed in more detail in the publications related to this project.

- The ensembles of climate change projections used for the extreme flood and flood risk analyses contain a total of 18 members. This is the largest ensemble of climate model simulations yet for flood risk analysis in the Rhine basin. However, its size (18 members) still makes the selection of a theoretical distribution to describe the PDF of risk difficult. Future research should aim to expand the number of climate model members, and where possible increase the number of parent GCMs used in the RCM ensemble.

- Probabilistic projections start with having high quality climate ensembles available. Much climate modelling research is focused on improving individual models [IPCC, 2007b]. More research is needed to construct equilibrated climate model ensembles that can be used for hydrological and subsequently flood risk analyses.

- The climate projections used are all for the IPCC A1B scenario, since the most model runs are available for this scenario. Future studies should aim to cover a larger range of emission scenarios; new GCM simulations currently being carried out for the Fifth Assessment Report (AR5) of the IPCC may facilitate such studies.

- Climate models make future projections based on changes in greenhouse gas concentrations. However, natural climate variability also has a large influence on extreme river discharges [Ward et al., 2010]. More research is needed on how flood risk is affected by natural climate variability, as variability could exacerbate/ameliorate climate change impacts in the near future [Swanson et al 2009]. For example it would be useful to use several realisations from each GCM or RCM.

- Flood estimates based on long resampled precipitation and temperature series are also prone to natural variability. For the Meuse basin this has been explored by resampling from different sub-series of the historical data [Kramer et al., 2008; Leander and Buishand, 2008]. A similar study is planned for the Rhine basin.

- The limited length of the resampled sequences causes a random error in the flood risk estimates. Therefore it may be useful to study the sensitivity of these estimates to the length of the resampled sequences. The error in the 1250-year discharge due to the limited simulation length has been quantified for the river Meuse (Leander, 2009), but for an empirical quantile estimate rather than the Weissman estimate.

- The GCM time-series have been downscaled using the delta-change approach. This approach is useful as it is relatively cheap and it incorporates the observations, but it also has several limitations. It does not use physics for processes on smaller scales, only changes in statistical properties. Some potentially influential feedbacks are not incorporated. The method also has many degrees of freedom. Most of these were tested carefully, and choices were made based on expert opinions or literature, but still the change between the resampled observations and the transformed resampled observations has to be interpreted with care.

- The RCM simulations have been bias corrected. This correction is uncertain for extreme daily precipitation amounts. It is further assumed that the same correction applies to the control and future simulations. In future studies it would be preferable to assess the change in discharge quantiles for the RCM simulations based on the control simulation of each RCM (rather than using the observations as the reference).

- The HBV-96 hydrological model is calibrated based on historical data. Changes induced by climate change, for example changes in vegetation or groundwater levels, are not taken into account sufficiently; research is needed to develop more climate-robust hydrological models.

- In this research, no hydrodynamic model was used. Hence, it is assumed that no upstream inundation takes place. The values for extreme discharges presented will therefore generally be overestimations.

- We have developed a simple inundation model and coupled it to a flood damage model. The simplifications dictate the method's applications. The Floodscanner method is not intended to replace the need for hydraulic modelling with more complex models. Flood damage estimates at fine resolutions need to employ more state-of-the-art methods [e.g. Ernst et al., 2010]. However, the use of such detailed models is not feasible in studies requiring large number of inundation scenarios over large areas. Our research shows that more attention is needed on the development of relatively simple inundation models. The method developed and applied here is capable of this, but refinements could be added to include the most important physical processes in a relatively simple manner. In future studies it may be useful to first employ a method such as Floodscanner to identify which return periods have the most important influence on the risk estimate. Once these have been established, it may still be preferential to employ a more complex process-based model to simulate inundation for a selected number of return-periods [Ward et al., 2011a, 2011b].

- Since one of the main aims of the present study is to demonstrate a framework for producing probabilistic flood risk estimates, we do not examine other sources of uncertainty. At each stage of the modelling process, large uncertainties can be introduced, and a full flood risk assessment should attempt to assess their influence on the final risk estimates [Apel et al., 2004]. Future research should attempt to estimate the uncertainty associated with the different parts of the model chain and input data [e.g. De Moel and Aerts, 2011].

- Moreover, we only present a probabilistic flood risk scenario under climate change. In reality, flood risk is also affected by many other factors (such as land subsidence, land use change, and population growth) which should also be examined in future research.

- Coping with climate change requires the undertaking of various adaptation measures to limit the projected rise in flood risk. The effectiveness of such adaptation measures in preventing flood damage could be evaluated using a probabilistic flood-risk framework. However, we were specifically requested to concentrate on scientific methods for risk estimation, rather than research on how to use the methods and/or framework for assessing adaptation options. Future research should examine both how the methods developed here can be applied to improve adaptation planning and decision-making; how decision-makers use the results of probabilistic impacts assessments; and how the information provided by probabilistic flood risk estimates can most effectively be communicated to stakeholders.

7. Conclusions

We present a first attempt to demonstrate a framework for producing probabilistic estimates of flood risk. We simulated discharge, flood damage, and flood risk for current conditions and for a future ensemble based on 18 climate model simulations (12 GCM simulations and six RCM simulations). For the extreme discharge quantiles, the bandwidths of the two ensembles are similar at Lobith and Cologne, but the bandwidth of the RCM ensemble is smaller than that of the GCM ensemble at Kaub. We found that extreme precipitation and discharge quantiles are, on average, lower for the RCM ensemble compared to the GCM ensemble. We found interesting spatial differences in the results. For example, the ensemble members do not cause the same changes in extreme discharge in all parts of the basin. This demonstrates the importance of using spatially distributed climate simulations in climate change impact studies.

We found relative change in winter half-year maximum 10-day basin-average precipitation to be a relatively good predictor of relative change in extreme discharge. However, in reality the relationship is complex, and also affected by factors such as temperature, evapotranspiration, snowmelt, soil moisture, groundwater levels, infiltration rates, flow routing, and land use. Nevertheless, the results suggest that, for the Rhine basin, change in multiday precipitation can give a first estimate of effects of changes in the discharge regime.

The availability of rapid inundation models is essential in a probabilistic flood risk modelling framework. The method applied here (Floodscanner) is capable of this, but refinements could be added to include the most important physical processes in a relatively simple manner.

We developed probabilistic flood risk scenarios for two case study sections of the Rhine, resulting in baseline flood risk estimates of € 60 million p.a. and € 5 million p.a. for the sections Bonn-Duisburg and Mainz-Koblenz respectively. The framework allows us to estimate the probability of future flood risk exceeding current risk (given the limitations of the study), namely 92% for the section Bonn-Duisburg and 96% for the section Mainz-Mosel. Using such a framework it is possible to assess the probability that flood risk will increase by any given factor, allowing for the assessment of risk under possible extreme future scenarios.

The research shows that the addition of the GCM ensemble to the existing RCM ensemble from RheinBlick 2050 leads to a slightly wider distribution of future flood risks estimates. However, the spread of the individual RCM and GCM ensembles is rather similar.

The research is intended to give a demonstration of the methods that can be used in a probabilistic flood risk framework; the absolute figures should be used for qualitative comparison only. Probabilistic flood risk assessments hold promise, but research remains to be carried out to: refine the methods presented here; examine how the methods can be applied to improve adaptation planning; assess how decision-makers use results of probabilistic impacts assessments; and to investigate how the information provided can most effectively be communicated to stakeholders.

8. References

Aerts, J.C.J.H. & W.J.W. Botzen, 2011. Climate change impacts on pricing long-term flood insurance: A comprehensive study for the Netherlands. Global Environmental Change, doi:10.1016/j.gloenvcha.2011.04.005.

Aerts, J.C.J.H., T. Sprong, & B.A. Bannik, 2008. Aandacht voor Veiligheid. Report number 009/2008. Amsterdam, Leven met Water, Klimaat voor Ruimte, DG Water.

Apel, H., A.H. Thieken, B. Merz & G. Blöschl, 2004. Flood risk assessment and associated uncertainty. Natural Hazards and Earth System Sciences, 4, 295-308.

Apel, H., A.H. Thieken, B. Merz & G. Blöschl, 2006. A probabilistic modelling system for assessing flood risks. Natural Hazards, 38, 79-100, doi:10.1007/s11069-005-8603-7.

Apel, H., B. Merz & A.H. Thieken, 2008. Quantification of uncertainties in flood risk assessments. International Journal of River Basin Management, 6, 149-162.

Apel, H., G.T. Aronica, H. Kreibich & A.H. Thieken, 2009. Flood risk analyses-how detailed do we need to be? Natural Hazards, 49, 79-98, doi:10.1007/s11069-008-9277-8.

Beersma, J.J., T.A. Buishand, & R. Wójcik, 2001. Rainfall generator for the Rhine basin: multi-site simulation of daily weather variables by nearest-neighbour resampling. International Commission for the Hydrology of the Rhine Basin (CHR). CHR-Report No. I-20.

Boos, D.D., 1984. Using extreme value theory to estimate large percentiles. Technometrics, 26, 33-39.

Botzen, W.J.W. & J.C.J.M. van den Bergh, 2008. Insurance against climate change and flooding in the Netherlands: Present, future, and comparison with other countries. Risk Analysis, 28(2), 413-426.

Botzen, W.J.W. & J.C.J.M. van den Bergh, 2009. Bounded rationality, climate risks and insurance: Is there a market for natural disasters? Land Economics, 85(2), 266-279.

Bouwer, L.M., 2010. Have disaster losses increased due to anthropogenic climate change?, Bulletin of the American Meteorological Society, 92, 39-46, doi:10.1175/2010BAMS3092.1.

Bouwer, L.M., P. Bubeck, A.J. Wagtendonk & J.C.J.H. Aerts, 2009. Inundation scenarios for flood damage evaluation in polder areas. Natural Hazards and Earth System Sciences, 9, 1995-2007, doi:10.5194/nhess-9-1995-2009.

Bouwer, L.M., P. Bubeck & J.C.J.H. Aerts, 2010. Changes in future flood risk due to climate and development in a Dutch polder area. Global Environmental Change, 20, 463-471, doi:10.1016/j.gloenvcha.2010.04.002.

Braca, G., 2008. Stage-discharge relationships in ocean channels: practices and problems. Trento, Università degli Studi di Trento, Dipartimento di Ingegneria Civile e Ambientale. FORALPS Technical Report 11.

Bronstert, A., D. Niehoff & G. Bürger, 2002. Effects of climate and land-use change on storm runoff generation: present knowledge and modelling capabilities. Hydrological Processes, 16, 509-529, doi:10.1002/hyp.326, 2002.

Buishand, T.A. & T. Brandsma, 2001. Multisite simulation of daily precipitation and temperature in the Rhine Basin by nearest-neighbor resampling. Water Resources Research, 37, 2761-2776, doi:10.1029/2001wr000291.

De Moel, H. & J.C.J.H. Aerts, 2011. Effect of uncertainty in land use, damage curves and inundation depth on flood damage estimates. Natural Hazards, 58(1), 407-425, doi:10.1007/s11069-010-9675-6.

Ernst, J., B. Dewals, S. Detrembleur, P. Archambeau, S. Erpicum, & M. Pirotton, 2010. Micro-scale flood risk analysis based on detailed 2D hydraulic modelling and high resolution geographic data. Natural Hazards, 55, 181-209, doi:10.1007/s11069-010-9520-y.

Few, R., 2003. Flooding, vulnerability and coping strategies: local responses to a global threat. Progress in Development Studies, 3, 43-58.

Fowler, H.J., M. Ekström, C.G. Kilsby & P.D. Jones. 2005. New estimates of future changes in extreme rainfall across the UK using regional climate model integrations. 1: assessment of control climate. Journal of Hydrology, 300, 212-233.

Fowler H, S. Blenkinsop, C. & Tebaldi, 2007. Linking climate change modelling to impacts studies: recent advances in downscaling techniques for hydrological modelling. International Journal of Climatology, 27, 1547-1578.

Froot, K.A. 1999. The financing of catastrophe risk. Chicago, University of Chicago Press.

Garrett, C. & P. Müller, 2008. Extreme events. Bulletin of the American Meteorological Society, 89(11), 133.

Gaslikova, L., A. Schwerzmann, C.C. Raible & T. F. Stocker, 2011. Future storm surge impacts on insurable losses for the North Sea region. Natural Hazards and Earth System Sciences, 11, 1205-1216, doi:10.5194/nhess-11-1205-2011.

Görgen, K., J. Beersma, G. Brahmer, H. Buiteveld, M. Carambia, O. de Keizer, P. Krahe, E. Nilson, R. Lammersen, C. Perrin & D. Volken, 2010. Assessment of Climate Change Impacts on Discharge in the Rhine River Basin: Results of the RheinBlick 2050 Project. International Commission for the Hydrology of the Rhine Basin (CHR), CHR-Report No. I-23.

Gouldby, B. & G. Kingston, 2007. Uncertainty and sensitivity analysis method for flood risk analysis. Wallingford, HR Wallingford. FLOODsite Report Number. T024-10-07.

Grossi, P. & H.C. Kunreuther, 2006. Models for hard times. Contingencies. March/April 2006, 33-36.

Hall, J., 2007. Probabilistic climate scenarios may misrepresent uncertainty and lead to bad adaptation decisions. Hydrological Processes, 21, 1127-1129.

Hall, J., G. Fu & J. Lawry, 2007 Imprecise probabilities of climate change: aggregation of fuzzy scenarios and model uncertainties. Climatic Change, 81, 265-281, doi:10.1007/s10584-006-9175-6.

Haylock, M.R., G.C. Cawley, C. Harpham, R.L. Wilby & C.M. Goodess, 2006. Downscaling heavy precipitation over the United Kingdom: a comparison of dynamical and statistical methods and their future scenarios. International Journal of Climatology, 26, 1397-1415, doi:10.1002/joc.1318.

Hilferink, M. & P. Rietveld, 1999. Land Use Scanner: an integrated GIS model for long term projections of land use in urban and rural areas. Journal of Geographical Systems, 1, 155–177. doi:10.1007/s101090050010.

Hurkmans, R., W. Terink, R. Uijlenhoet, P. Torfs, D. Jacob & P.A. Troch, 2010. Changes in streamflow dynamics in the Rhine Basin under three high-resolution regional climate scenarios. Journal of Climate, 23, 679-699, doi: 10.1175/2009JCLI3066.1.

ICPR, 2001. Atlas 2001. Atlas of flood danger and potential damage due to extreme floods of the Rhine. Koblenz, International Commission on the Protection of the Rhine (ICPR).

ICPR, 2005. Action Plan on Floods. Koblenz, International Commission on the Protection of the Rhine (ICPR).

IPCC, 2007a. Climate Change 2007. Impacts, Adaptation and Vulnerability. Contribution of Working Group II to the Fourth Assessment Report of the Intergovernmental Panel on Climate Change. Cambridge, Cambridge University Press.

IPCC, 2007b. Climate Change 2007. The Physical Science Basis. Contribution of Working Group I to the Fourth Assessment Report of the Intergovernmental Panel on Climate Change. Cambridge, Cambridge University Press.

Jarvis A., H.I. Reuter, A. Nelson & E. Guevara, 2006. Hole-filled seamless SRTM data V3. International Centre for Tropical Agriculture (CIAT), available from http://srtm.csi.cgiar.org.

Jonkeren, O.E., 2009. Adaptation to climate change in inland waterway transport, Amsterdam, VU University Amsterdam. Ph.D. thesis.

Kendon, E.J., R.G. Jones, E. Kjellström & J.M. Murphy, 2010. Using and Designing GCM-RCM Ensemble Regional Climate Projections. Journal of Climate, 23, 6485-6503, doi:10.1175/2010JCLI3502.1.

Klijn, F., P.J.A. Baan, K.M. de Bruijn & J. Kwadijk, 2007. Overstromingsrisico's in Nederland in een veranderend klimaat. Delft, WL|Delft hydraulics, Report Q4290.

Kramer, N., J. Beckers & A. Weerts, 2008. Generator of rainfall and discharge extremes (GRADE) – part D & E. Delft, Deltares, Deltares report Q4424.

Kron, W., 2005. Flood Risk = Hazard • Values • Vulnerability. Water International, 30, 58-68.

Kwadijk, J.C.J., 1993. The impact of climate change on the discharge of the River Rhine. University of Utrecht, The Netherlands. Ph.D. thesis.

Kwadijk, J.C.J. & H. Middelkoop, 1994. Estimation of impact of climate change on the peak discharge probability of the river Rhine. Climatic Change, 27, 199–224.

Landscan, 2008. LandScan 2008TM. High Resolution global Population Data Set copyrighted by UT-Battelle, LLC, operator of Oak Ridge National Laboratory under Contract No. DE-AC05-00OR22725 with the United States Department of Energy. The United States Government has certain rights in this Data Set. Neither UT-BATTELLE, LLC NOR THE UNITED STATES DEPARTMENT OF ENERGY, NOR ANY OF THEIR EMPLOYEES, MAKES ANY WARRANTY, EXPRESS OR IMPLIED, OR ASSUMES ANY LEGAL LIABILITY OR RESPONSIBILITY FOR THE ACCURACY, COMPLETENESS, OR USEFULNESS OF THE DATA SET.

Leander, R., 2009. Simulation of precipitation and discharge extremes of the river Meuse in current and future climate. University of Utrecht, The Netherlands. Ph.D. thesis.

Leander, R. & T.A. Buishand, 2007. Resampling of regional climate model output for the simulation of extreme river flows. Journal of Hydrology, 332(3-4), 487-496.

Leander, R. & T.A. Buishand, 2008. Rainfall generator for the Meuse basin: Description of 20 000-year simulations. De Bilt, Royal Netherlands Meteorological Institute (KNMI), KNMI-publication 196-IV.

Leander, R., T.A. Buishand, B.J.J.M. van den Hurk & M.J.M. de Wit, 2008. Estimated changes in flood quantiles of the river Meuse from resampling of regional climate model output. Journal of Hydrology, 351, 331-343.

Lenderink, G., A. Buishand & W. van Deursen, 2007. Estimates of future discharges of the river Rhine using two scenario methodologies: direct versus delta approach. Hydrology and Earth System Sciences, 11, 1145-1159.

Manning, L.J., J.W. Hall, H.J. Fowler, C.G. Kilsby. & C. Tebaldi, 2009. Using probabilistic climate change information from a multimodel ensemble for water resources assessment. Water Resources Research, 45, W11411, doi:10.1029/2007WR006674.

Maraun, D., F. Wetterhall, A. Ireson, R. Chandler, E. Kendon, M. Widmann, S. Brienen, H. Rust, T. Sauter & M. Themeßl, 2010. Precipitation downscaling under climate change. Recent developments to bridge the gap between dynamical models and the end user. Reviews of Geophysics, 48, 3.

Menzel, L., A.H. Thieken, D. Schwandt & G. Bürger, 2006. Impact of climate change on the regional hydrology – scenario-based modelling in the German Rhine catchment. Natural Hazards, 38, 45–61.

Merz, B., J. Hall, M. Disse & A. Schumann, 2010a. Fluvial risk management in a changing world. Natural Hazards and Earth System Sciences, 10, 509-527, doi:10.5194/nhess-10-509-2010.

Merz, B., H. Kreibich, R. Schwarze & A. Thieken, 2010b. Assessment of economic flood damage. Natural Hazards and Earth System Sciences, 10, 1697-1724, doi:10.5194/nhess-10-1697-2010.

Meyer, V., D. Haase & S. Scheuer, 2009. Flood risk assessment in European river basins - concept, methods, and challenges exemplified at the Mulde River. Integrated Environmental Assessment and Management, 5, 17-26, doi:10.1897/IEAM_2008-031.1.

Michel-Kerjan, E.O. 2008. Toward a new risk architecture: The question of catastrophe risk calculus. Social Research 75(3), 819-854.

Middelkoop, H., K. Daamen, D. Gellens, W. Grabs, J.C.J. Kwadijk, H. Lang, B.W.A.H. Parmet, B. Schädler, J. Schulla & K. Wilke, 2001. Impact of climate change on hydrological regimes and water resources management in the Rhine basin. Climatic Change, 49, 105-128.

Ministry of Transport, Public Works and Water Management, Province of Gelderland, Federal Institute of Hydrology, and Rijkswaterstaat, 2004. Grensoverschrijdende effecten van extreem hoogwater op de Niederrhein. Arnhem, The Netherlands.

New, M., A. Lopez, S. Dessai & R. Wilby, 2007. Challenges in using probabilistic climate change information for impact assessments: an example from the water sector. Philosophical Transactions of the Royal Society A, 365, 2117-2131, doi:10.1098/rsta.2007.2080.

Pittock A.B, R.N. Jones & C. Mitchell, 2001 Probabilities will help us plan for climate change - without estimates, engineers and planners will have to delay decisions or take a gamble. Nature. 413, 249-249, doi:10.1038/35095194.

Priestnall, G., J. Jaafar & A. Duncan, 2000. Extracting urban features from LiDAR-derived digital surface models. Computers, Environment and Urban Systems, 24, 65-78.

Prudhomme, C., N. Reynard & S. Crooks, 2002. Downscaling of global climate models for flood frequency analysis: where are we now? Hydrological Processes, 16, 1137-1150, doi:10.1002/hyp.1054.

Reilly, J., P.H. Stone, C.E. Forest, M.D. Webster, H.D. Jacoby & R.G. Prinn, 2001. Uncertainty in climate change assessments. Science, 293, 430–433.

Rougier, J., 2007. Probabilistic inference for future climate using an ensemble of climate model evaluations. Climatic Change, 81-247-264, doi:10.1007/s10584-006-9156-9.

Shabalova, M.V., W.P.A. van Deursen & T.A. Buishand, 2003. Assessing future discharge of the River Rhine using regional climate model integrations and a hydrological model. Climatic Research, 23, 233-246.

Swanson, K.L., G. Sugihara & A.A. Tsonis. 2009. Long-term natural variability and 20th century climate change. Proceedings of the National Academy of Sciences, 106, 38, doi:10.1073/pnas.0908699106.

Tebaldi, C. & D.B. Lobell, 2008. Towards probabilistic projections of climate change impacts on global crop yields. Geophysical Research Letters, 35, L08705, doi:10.1029/2008GL033423.

Tebaldi, C., L.O. Mearns, D. Nychka & R.L. Smith, 2004. Regional probabilities of precipitation change: A Bayesian analysis of multimodel simulations. Geophysical Research Letters, 31, L24213, doi:10.1029/2004GL021276.

Te Linde, A.H., J.C.J.H. Aerts, A.M.R. Bakker & J.C.J. Kwadijk, 2010. Simulating low probability peak discharges for the Rhine basin using resampled climate modeling data. Water Resources Research, 46, W03512, doi:10.1029/2009WR007707.

Te Linde, A.H., P. Bubeck, J.E.C. Deckers, H. de Moel & J.C.J.H. Aerts, 2011. Future flood risk estimates along the river Rhine. Natural Hazards and Earth System Sciences, 11, 459-473, doi:10.5194/nhess-11-459-2011.

Thieken, A.H., A. Olschewski, H. Kreibich, S. Kobsch & B. Merz, 2008. Development and evaluation of FLEMOps – a new Flood Loss Estimation MOdel for the private sector, in: Proverbs, D., C. Brebbia & E. Penning-Roswell (eds.). Flood Recovery, Innovation and Response I. Ashurst, WIT Press.

Tunstall, S.M., C.L. Johnson & E.C. Pennning Rowsell, 2004. Flood Hazard Management in England and Wales: From Land Drainage to Flood Risk Management. Proceedings of the World Congress on Natural Disaster Mitigation. New Delhi, India.

Van de Langemheen, W. & H.E.J. Berger, 2001. Hydraulische randvoorwaarden 2001: maatgevende afvoeren Rijn en Maas. RIZA report number 2002.014. Arnhem, Rijksinstituut voor Integraal Zoetwaterbeheer en Afvalwaterbehandeling.

Van den Hurk, B., A. Klein Tank, G. Lenderink, A. van Ulden, A., G. van Oldenborgh, C. Katsman, H. van den Brink, F. Keller, J. Bessembinder, G. Burgers, G. Komen, W. Hazeleger & S. Drijfhout, 2006. KNMI Climate Change Scenarios 2006 for the Netherlands. Report number WR 2006-01, De Bilt, KNMI.

Van den Hurk, B., A. Klein Tank, G. Lenderink, A. van Ulden, A., G. van Oldenborgh, C. Katsman, H. van den Brink, F. Keller, J. Bessembinder, G. Burgers, G. Komen, W. Hazeleger & S. Drijfhout, 2007. New climate change scenarios for the Netherlands. Water Science and Technology, 56(4), 27-33, doi: 10.2166/wst.2007.533.

Van der Linden, P. & J. Mitchell, 2009. ENSEMBLES: Climate change and its impacts: Summary of research and results from the ENSEMBLES project. Exeter, Met Office Hadley Centre.

Van Pelt, S.C., B.J.J.M. van den Hurk, T.A. Buishand & J.J. Beersma, 2011a. Improving the probability distribution of the change in extreme river flows due to climate change. De Bilt, KNMI. Unpublished document.

Van Pelt, S.C., B.J.J.M. van den Hurk, T.A. Buishand & P. Kabat, 2011b. Improving the probability distribution of the change in extreme river flows due to climate change. EGU General Assembly 2011, Geophysical Research Abstracts, 13, EGU2011-9106. 5 April 2011, Vienna, Austria.

Van Pelt, S.C., J.J. Beersma, T.A. Buishand, B.J.J.M. van den Hurk & O. de Keizer, in prep. Evaluation of the probability distribution of the future change in extreme precipitation. Scientific manuscript to be submitted in 2012.

Vis, M., F. Klijn, K.M. de Bruijn & M. van Buuren, 2003. Resilience strategies for flood risk management in the Netherlands. International Journal of River Basin Management, 1, 33-40.

Ward, R.C. & M. Robinson, 1990. Principles of hydrology. London, McGraw-Hill Book Company.

Ward, P.J., W. Beets, L.M. Bouwer & J.C.J.H. Aerts, 2010. Sensitivity of river discharge to ENSO. Geophysical Research Letters, 37, L12402. doi:10.1029/2010GL043215.

Ward, P.J., H. de Moel & J.C.J.H. Aerts, 2011a. How are flood risk estimates affected by the choice of return-periods? Natural Hazards and Earth System Sciences, 11, 3181-3195, doi:10.5194/nhess-11-3181-2011.

Ward, P.J., H. de Moel & J.C.J.H. Aerts, 2011b. Rapid damage modelling for probabilistic risk estimation: example from the Meuse in Dutch Limburg. Amsterdam, Institute for Environmental Studies (IVM), VU University Amsterdam. IVM Report number W11-08.

Ward, P.J., H. Renssen, J.C.J.H. Aerts & P.H. Verburg, 2011c. Sensitivity of discharge and flood frequency to twenty-first century and late Holocene changes in climate and land use (River Meuse, northwest Europe). Climatic Change, 106, 179-202, doi:10.1007/s10584-010-9926-2.

Ward, P.J., J.C.J.H. Aerts, B.J.J.M. van den Hurk, O. de Keizer & S.C. van Pelt, 2011d. Flood risk estimation using probabilistic climate change scenarios. Abstract D-1-207. 5th International Conference on Flood Management (ICFM5), 27-29 September 2011, Tokyo, Japan.

Ward, P.J., S.C. van Pelt, O. de Keizer, J.C.J.H. Aerts, J.J. Beersma, B.J.J.M. van den Hurk & A.H. Te Linde, in review. Probabilistic flood risk assessment. Submitted to Journal of Flood Risk Management.

Webster, M.D., 2003. Communicating climate change uncertainty to policy-makers and the public. Climatic Change, 61, 1-8.

Weissman, I., 1978. Estimation of parameters and large quantiles based on the k largest observations. Journal of the American Statistical Association, 73, 812-815.

Wind, H.G., T.M. Nieron, C.J. de Blois & J.L. de Kok, 1999. Analysis of flood damages from the 1993 and 1995 Meuse floods. Water Resources Research, 35, 3459-3465.

Wójcik, R., J.J. Beersma & T.A. Buishand, 2000. Rainfall generator for the Rhine basin: multi-site generation of weather variables for the entire drainage area. De Bilt, KNMI, Publication 186-IV.

Woodhead, S., N. Asselman, Y. Zech, S. Soares-Frazão, P. Bates & A. Kortenhaus, 2007. Evaluation of inundation models. Delft, WL | Delft Hydraulics, Report number T08-07-01.

Young, K.C., 1994. A multivariate chain model for simulating climatic parameters from daily data. Journal of Applied Meteorology, 33, 661-671.

Climate changes Spatial Planning

Climate change is one of the major environmental issues of this century. The Netherlands are expected to face climate change impacts on all land- and water related sectors. Therefore water management and spatial planning have to take climate change into account. The research programme 'Climate changes Spatial Planning', that ran from 2004 to 2011, aimed to create applied knowledge to support society to take the right decisions and measures to reduce the adverse impacts of climate change. It focused on enhancing joint learning between scientists and practitioners in the fields of spatial planning, nature, agriculture, and water- and flood risk management. Under the programme five themes were developed: climate scenarios; mitigation; adaptation; integration and communication. Of all scientific research projects synthesis reports were produced. This report is part of the Adaptation series.

Adaptation

Dutch climate research uses a 'climate proofing' approach for adaptation. Climate proofing does not mean reducing climate based risks to zero; that would be an unrealistic goal for any country. The idea is to use a combination of infrastructural, institutional, social and financial adaptation strategies to reduce risk and optimalise opportunities for large scale innovations. Climate changes Spatial Planning realised projects in a multidisciplinary network that jointly assessed impacts and developed adaptation strategies and measures. The following themes were central to the programme: water safety, extreme precipitation, nature and biodiversity, agriculture, urban areas, transport (inland and road transport) and the North Sea ecosystem. In special projects, the so called hotspots, location-specific measures were developed that focused on combining 'blue', 'green' and 'red' functions.

www.climatechangesspatialplanning.nl